Mapping diluents for water-lean solvents: a parametric study

Ricardo R. Wanderley, Hanna K. Knuutila*

Department of Chemical Engineering, Norwegian University of Science and Technology (NTNU), NO-7491 Trondheim, Norway

Abstract

Water-lean solvents are typically defined as mixtures between an organic diluent and an amine. These solvents are thought to deliver potential benefits in CO_2 capture systems, such as enhanced mass transfer properties, increased absorption capacities and lower regeneration heat duties. However, it is yet unclear what properties of the organic diluent one should aim for when developing these solvents. For example, while it is understood that high CO_2 physical solubility is desirable if one wants to enhance mass transfer rates, the contributions of viscosity and electrostatic properties (e.g. dielectric permittivity) are still uncertain. Simultaneously, as low vapor pressures are interesting for reducing latent heat duties in the regeneration process, the effects of viscosity and thermal conductivity in the cross-heat exchanger before the reboiler are often neglected or underestimated. This work aims to address such deficiencies by carrying an explicit analysis, based on rigorous modelling, on the influences of each individual parameter of the organic solvent when mixed with monoethanolamine as a token amine. The contributions of CO_2 solubility, viscosity, dielectric permittivity, heat capacity, thermal conductivity and vapor pressure to the performances in the absorber and the desorber are exhaustively discussed. Finally, an overall assessment on which properties are effectively desirable in a water-lean solvent is performed, as well as some predictions on which kinds of challenges these solvents will have to face upon implementation.

Keywords: CO2 absorption, water-lean solvents, hybrid solvents, modelling, parametric study

1. Introduction

Water-lean solvents have been often proposed as interesting alternatives to regular aqueous amine solvents for CO_2 capture applications[1–6]. Due to the multitude of possibilities regarding water-lean solvent formulation, the issue of coming up with a brand-new solvent may be as cumbersome as blindly guessing which chemicals to put together. To address this complexity,

* Correspondence: hanna.k.knuutila@ntnu.no

the present study provides a qualitative and, to certain extent, quantitative evaluation of what parameters one should keep in mind when looking for candidates for water-lean solvents.

Before carrying this parametric evaluation, a short discussion on which advantages water-lean solvents can really bring to the table is warranted. Some authors have proposed that the capacity for CO_2 absorption in water-lean solvents would be extended due to their coupling of physical and chemical absorption[3,7,8]. However, in previous experiments carried by this group and others[9–11], this was not observed to be the case for low-to-moderate CO_2 partial pressure spans (0–600 kPa). Clearly, any advantages brought by this supposed extended absorption capacity will hardly be yielded in regular post-combustion CO_2 capture applications, where CO_2 partial pressures are typically lower than 600 kPa.

Additionally, some authors have proposed that either the heat of absorption or the reboiler heat duties can be considerably lower in water-lean solvents[3,4,12]. Our previous research has showed that the heat of absorption, when employing monoethanolamine-based (MEA-based) water-lean solvents, is roughly the same as with aqueous solvents[10]. This does not contradict the studies which proposed that this should be the case for secondary or hindered amines[4,12], but it suggests that one should not take for granted that carbamate-forming amines will deliver reboiler duty savings through heat of absorption alone. In our previous work[10], we have indicated that the reboiler duty savings might come from the low volatility of some organic diluents used in water-lean solvent formulation (N-methyl-2-pyrrolidone, monoethylene glycol, tetrahydrofurfuryl alcohol) providing less vaporization heat expenditures in the reboiler, something which seems to be in agreement with literature[13].

Parallelly, some authors suggested that the shifting from aqueous to water-lean solvents can increase mass transfer rates in the absorber[6,9,14]. This enhancement in mass transfer rates is driven by increased CO_2 physical solubility, but depressed by increased viscosity, both of which are typical of water-lean solvents.

More recently, Yuan and Rochelle[15] have published a very interesting study on comparing aqueous solutions and their water-lean alternatives by looking at the thermodynamic efficiency of the CO_2 capture process with either type of absorbents. This efficiency was found to be related to a very definite set of diluent parameters, more precisely its viscosity, heat capacity and thermal conductivity.

This work takes inspiration in the parametric approach offered by Yuan and Rochelle[15], but focuses on more immediate issues regarding the practical applications of water-lean solvents.

We have narrowed this analysis onto two distinct areas of a prospective CO_2 capture plant, and into three different phenomena.

- In Section 2, the mass transfer rates in an isothermal absorber with potential water-lean solvents are investigated. We have employed rigorous penetration model calculations to assess the impacts of parameters such as diluent η (viscosity), H_A (Henry's coefficient for CO_2) and ε (diluent dielectric permittivity). As it is to be expected, there are clear trade-offs between viscosity and CO_2 solubility.
- In Section 3, we look at the thermal phenomena due to heat of absorption and diluent volatilization in an adiabatic absorber. We have employed equilibrium stage calculations in a MESH-type algorithm to quickly verify the impacts of parameters such as diluent C_P (heat capacity) and p^{sat} (saturation pressure). These parameters affect the temperature bulge locus and intensity in the absorber, the CO_2 capture capacity of the solvent and the loss of diluent through volatilization at the top of the column.
- In Section 4, the prospective reboiler heat duties are analyzed, determining the relevance of parameters such as diluent λ (heat conductivity), plus η, C_P and p^{sat} once again. We have carried this analysis through a simple evaluation of the performance of the cross-heat exchanger using a Nusselt model correlation, coupled with a shortcut evaluation of the reboiler heat duties with the equation proposed by Oexmann and Kather[16].

The studies carried in Sections 2, 3 and 4 may appear to have varying degrees of complexity, which is true. Nevertheless, their goal is fully complementary. With the analyses provided in these sections, one should be able to estimate the performance of a hypothetical water-lean solvent in the absorber based on the viscosity, CO_2 physical solubility, heat capacity and volatility of the *diluent*, while an estimation of reboiler heat duties can be derived from the aforementioned parameters plus the heat conductivity of the *diluent* again. Notwithstanding their varying complexities, all of our analyses are in service of aiding researchers on water-lean solvents to better understand the contributions of each individual parameter to the overall performance of a CO_2 capture plant.

In Section 5, some issues on chemical reactivity between solvent and amine stretching farther from a simple parametric analysis will be discussed briefly, since this discussion also aids the selection of proper diluents. Finally, Section 6 is for conclusions.

It is important to highlight, finally, that this study is invested in analyzing parameters relevant to the formulation of water-lean solvents that rely on *carbamate formation*. For water-lean solvents based on different reaction routes, such as those proposed by Barzagli et al.[17], the analysis outlined in Section 2 is rigorously not valid, though some insights might be granted from the results obtained in Sections 3 and 4.

2. Mass transfer properties in an isothermal absorber

The enhancement of mass transfer rates in water-lean solvents is one of the most promising factors guiding the studies on this brand of solvents. This enhancement comes as a trade-off between increased CO_2 physical solubilities and viscosities, both having opposite effects on the overall mass transfer rates. The fact that organic diluents often have viscosities superior to that of water highlights the importance of better understanding this trade-off.

However, there are several other factors in play when assessing the mass transfer properties. For example, CO_2 loading has a different impact in aqueous and in water-lean solvents due to diverse electrostatic phenomena: its effects on viscosity[10], as well as on salting-out[9], are felt the harder the lower the dielectric permittivity of the milieu. Similarly, kinetics[18–20] and reaction equilibria[14] experience a change in water-lean solvents that might have an understated relevance in past studies, especially considering that the increased viscosity of these solvents might lead to amine depletion in the gas-liquid interface.

This Section 2 will provide a deep analysis on all these effects. This is clearly the most sophisticated analysis of the three carried in this work, a fact that comes out of necessity – mass transfer phenomena are simply too complex to properly investigate in any other meaningful way. The ultimate goal is Section 2.8, which will finally assess the trade-off between CO_2 solubility and diluent viscosity as a function of the dielectric permittivity ε. Before that, Sections 2.1–2.6 lay the groundwork for the final conclusion, while Section 2.7 extends the theoretical analysis to a number of real candidates for water-lean solvent formulation.

2.1. What affects mass transfer rates in water-lean solvents

The most straightforward way of evaluating the impact that each parameter has on mass transfer rates is by considering the penetration of CO_2 into the solvent upon contact between vapor and liquid phases[21,22]. By doing this, we are assured that no significant phenomena (e.g. solvent depletion in the interface, shifting in reaction orders) will be overlooked.

Following this approach, CO_2 concentration in the vapor-liquid interface is constrained by the thermodynamical equilibrium dictated by Henry's law for dilute components. In the liquid bulk, diffusion of CO_2 is followed by its reaction with amine molecules, forming carbamate and protonated base according to Reactions (R1) and (R2). These reactions constitute the so-called *zwitterion mechanism*[23]. There is an ongoing debate in literature regarding whether the zwitterion mechanism correctly represents the real phenomena behind the reaction between CO_2 and aminet[24]. Regardless, the rate equations obtained by employing the zwitterion mechanism can be shown to give results consistent with those derived by consideration of the one-step termolecular mechanism[25,26]. Furthermore, the reasons for choosing the zwitterion mechanism in our approach will be evidenced briefly in Section 2.3.

$$CO_2 + Am \underset{k_{-1}}{\overset{k_2}{\rightleftharpoons}} Am^+COO^- \qquad \text{(R1)}$$

$$Am^+COO^- + B \xrightarrow{k_b} AmCOO^- + BH^+ \qquad \text{(R2)}$$

One can consider Reactions (R1) and (R2) to derive an expression for the reaction rate of CO_2. Typically, the strongest base in solution will be the amine itself, and so this will be the preferable reactant, B, in Reaction (R2). Furthermore, the zwitterion is an unstable molecule and its concentration can be approximated by zero at all times. This results in the reaction rate expression given by Eq. (1), where A = CO_2, B = amine, C = carbamate and D = protonated amine (notice that $C_C = C_D$, so that C_D will always be omitted in the following equations).

$$r_A = -\frac{\frac{k_2 \cdot k_b}{k_{-1}} \cdot C_A \cdot {C_B}^2}{1 + \frac{k_b}{k_{-1}} \cdot C_B} \qquad (1)$$

Eq. (1) gives an expression for the irreversible reaction between CO_2 and amine forming carbamate and protonated amine. For more general uses, however, it is interesting to consider that the conversion might be bounded by chemical equilibrium. This can be easily taken into account by modifying Eq. (1) into Eq. (2).

$$r_A = -\frac{\frac{k_2 \cdot k_b}{k_{-1}} \cdot \left(C_A \cdot {C_B}^2 - \frac{1}{K} \cdot {C_C}^2\right)}{1 + \frac{k_b}{k_{-1}} \cdot C_B} \qquad (2)$$

The reaction rate expressions for amine and carbamate come directly from stoichiometric relationships, so that $r_B = 2 \cdot r_A$ and $r_C = -r_A$. The penetration equation for an arbitrary component i is then given by Equation (3), where r_i is the reaction rate of component i.

$$\frac{\partial C_i}{\partial t} = D_i \cdot \frac{\partial^2 C_i}{\partial x^2} + r_i \tag{3}$$

Substituting for A, B and C results in Eq. (4).

$$\frac{\partial C_A}{\partial t} = D_A \cdot \frac{\partial^2 C_A}{\partial x^2} - \frac{\frac{k_2 \cdot k_b}{k_{-1}} \cdot \left(C_A \cdot {C_B}^2 - \frac{1}{K} \cdot {C_C}^2 \right)}{1 + \frac{k_b}{k_{-1}} \cdot C_B} \tag{4a}$$

$$\frac{\partial C_B}{\partial t} = D_B \cdot \frac{\partial^2 C_B}{\partial x^2} - 2 \cdot \frac{\frac{k_2 \cdot k_b}{k_{-1}} \cdot \left(C_A \cdot {C_B}^2 - \frac{1}{K} \cdot {C_C}^2 \right)}{1 + \frac{k_b}{k_{-1}} \cdot C_B} \tag{4b}$$

$$\frac{\partial C_C}{\partial t} = D_B \cdot \frac{\partial^2 C_C}{\partial x^2} + \frac{\frac{k_2 \cdot k_b}{k_{-1}} \cdot \left(C_A \cdot {C_B}^2 - \frac{1}{K} \cdot {C_C}^2 \right)}{1 + \frac{k_b}{k_{-1}} \cdot C_B} \tag{4c}$$

For our algorithm, the expression related to the transport of protonated amine is omitted. This is because no other charged product is created in our approach other than the carbamate and the protonated amine itself. Since both products are formed simultaneously ($C_C = C_D$), and since one has to impose electrostatic equilibrium to the solvent at all times, the diffusivity of protonated amine and that of carbamate must be equal, and an expression for one shall have the same form as the expression for the other. Therefore, Eq. (4c) accounts for the transport of both products. Furthermore, an approximation taken in this work is assuming that the diffusivity of these products is similar to that of the amine itself ($D_C \approx D_B$). This is in accordance with the approach adopted by several other studies[21,27].

The resolution of Eq. (4) requires two sets of boundary conditions, one for the interface and another for the liquid bulk, plus one set of initial conditions. The initial conditions are ordinarily given by setting the initial concentrations of all components before absorption homogeneously throughout the whole liquid solvent, as seen on Eq. (5).

$$C_A|_{t=0,\forall x} = C_{A,i} \tag{5a}$$

$$C_B|_{t=0,\forall x} = C_{B,i} \tag{5b}$$

$$C_C|_{t=0,\forall x} = C_{C,i} \tag{5c}$$

In the interface, one can assume that the concentration of CO_2 is in equilibrium with the partial pressure of CO_2 in the vapor phase by Henry's law and that there is no vaporization neither of amine nor products. This results in Eq. (6).

$$C_A|_{\forall t,x=0} = \frac{H_A}{p_A} \tag{6a}$$

$$\left.\frac{\partial C_B}{\partial x}\right|_{\forall t,x=0} = 0 \tag{6b}$$

$$\left.\frac{\partial C_C}{\partial x}\right|_{\forall t,x=0} = 0 \tag{6c}$$

In the liquid bulk, far from the interface at $x = \delta$, all the concentrations are the same as those before the absorption took place. This can be seen in Eq. (7).

$$C_A|_{\forall t,x=\delta} = \frac{H_A}{p_{A,i}} \tag{7a}$$

$$C_B|_{\forall t,x=\delta} = C_{B,i} \tag{7b}$$

$$C_C|_{\forall t,x=\delta} = C_{C,i} \tag{7c}$$

In conclusion, the system of partial differential equations outlined in Eq. (4) subject to the initial conditions Eq. (5) and the boundary conditions Eqs. (6) and (7) has to be integrated from $t = 0$ to $t = \tau$ and from $x = 0$ to $x = \delta$ so that one can obtain the concentration profiles of CO_2, amine and carbamate in the solvent. The integration limits are the absorption time τ and the penetration depth δ.

As one can see, with the aforementioned assumptions and approximations, the CO_2 mass transfer rates can be somewhat characterized by fixing two transport properties, two kinetic properties and two thermodynamical properties. These are:

- Transport properties: CO_2 diffusivity D_A and amine diffusivity D_B
- Kinetic properties: kinetic rate constant k_2 and kinetic rate constant ratio k_b/k_{-1}
- Thermodynamical properties: equilibrium coefficient K and Henry's coefficient H_A

These six parameters will be discussed further in the next sections. Before that, however, an explanation should be given about the equilibrium coefficient K. This property can be defined as by Eq. (8).

$$K = \frac{{C_C}^2}{C_A \cdot {C_B}^2} \tag{8}$$

As mentioned previously, in this work we are assuming that the only mechanisms through which CO_2 is absorbed are physical absorption and carbamate formation, i.e. no other CO_2 consuming reactions such as bicarbonate formation are taken into account. With this in mind, it is practical to discuss the equilibrium coefficient in terms of the loading α, which accounts for mols of CO_2 absorbed per mols of amine in solution. As a function of α, the concentrations of CO_2, amine and carbamate are given respectively by Eqs. (9), (10) and (11).

$$C_A = \frac{H_A}{p_A} \tag{9}$$

$$C_B = (1 - 2 \cdot \alpha) \cdot C_B^0 + 2 \cdot \frac{H_A}{p_A} \tag{10}$$

$$C_C = \alpha \cdot C_B^0 - \frac{H_A}{p_A} \tag{11}$$

Substituting Eqs. (9)–(11) in Eq. (8), one ends up with Eq. (12). This expression shows how to obtain the equilibrium coefficient K by employing α.

$$K = \frac{\left(\alpha \cdot C_B^0 - \frac{H_A}{p_A}\right)^2}{\frac{H_A}{p_A} \cdot \left[(1 - 2 \cdot \alpha) \cdot C_B^0 + 2 \cdot \frac{H_A}{p_A}\right]^2} \tag{12}$$

Finally, two of the properties shown previously are not characteristic of the solvent, but of the process or the algorithm itself. One of them is the penetration time τ. This property is equivalent to the surface renewal time scale, and in this study it has been fixed to a constant value obtained by using the Rocha et al. model[28,29] assuming an absorber working with structured packing of the type Intalox 2T (S = 0.0221 m, C_E = 0.9) and effective liquid phase velocity of U_e = 0.5 $m \cdot s^{-1}$. This results in a surface renewal time of $\tau \approx 0.05$ s. The second property is the penetration depth δ. This is the depth in which no more concentration gradient can be seen as one goes deeper into the solvent, i.e. all concentrations are those of the liquid bulk. It is important to fix this parameter at a value big enough so that the whole penetration profile can be obtained, but not so big as to jeopardize the speed and convergence of the calculations.

2.2. Mass diffusivity in water-lean solvents

Both CO_2 diffusivity and amine diffusivity are known to decrease with an increase in viscosity. In the case of CO_2, a simple way of representing this is by the famous Wilke-Chang correlation[30], which is expressed by Eq. (13).

$$D_A^0 = 7.4 \cdot 10^{-12} \cdot \frac{(\chi \cdot M)^{0.5} \cdot T}{\eta \cdot {V_A}^{0.6}} \tag{13}$$

In Eq. (14), the diffusivity D_A^0 in a certain unloaded solvent ($\alpha = 0$) can be obtained as a function of the molar volume of the solute at normal boiling point V_A ($V_A = 34.0$ cm^3·mol^{-1} for CO_2), the solvent's molecular weight M and viscosity η, its association parameter χ, and the process temperature T. The association parameter is related to how clustered together the solvent molecules are in a real solution, meaning $\chi = 1.0$ for ordinary non-associated solvents and $\chi = 2.6$ for a highly associated solvent such as water, which forms hydrogen bonds. Some organic liquids, such as methanol ($\chi = 1.9$) and ethanol ($\chi = 1.5$), have their association parameters reported in the original article by Wilke and Chang[30]. For other solvents, it is usually simpler and safer to assume that $\chi = 1.0$.

The Wilke-Chang correlation can be used for preliminary evaluation of the CO_2 diffusivity in water-lean solvents containing novel organic diluents. More than that, it gives an idea of how the diffusivity should decrease with viscosity for a fixed solvent, that is – by the power of 1. In other words, a consequence of the Wilke-Chang correlation is that Eq. (14) can be used to calculate the CO_2 diffusivity in a loaded solution ($\alpha > 0$) D_A by considering how the viscosity of this solution increases with loading and fixing $z = 1$.

$$D_A = D_A^0 \cdot \left(\frac{\eta^0}{\eta}\right)^z \tag{14}$$

More recently, the decrease of CO_2 diffusivity with viscosity in liquid solvents has been reported to follow the power of $z = 0.8$ by Versteeg and van Swaaij[31] and $z = 0.72$ by Dugas and Rochelle[32]. Regarding specifically the case of water-lean solvents, the value of $z = 0.524$ was obtained by Yuan and Rochelle[9] for NMP + MEA low-aqueous mixtures, who have proposed that CO_2 can diffuse inbetween molecular clusters despite increasing solvent viscosities at higher loadings.

The takeaway is that there is great uncertainty regarding how CO_2 diffusivity depends on viscosity. In the pragmatic point of view, the values of $z = 0.8$ or 0.72 are more firmly stablished

in the literature, and the latter will be used for evaluating how D_A varies with η (and consequently with α).

Meanwhile, we have adopted the approach suggested by Park et al.[33] and Hwang et al.[34] for calculating the amine diffusivity D_B^0 in unloaded water-lean solvents. This approach consists in adapting the amine diffusivity from aqueous to water-lean based on how CO_2 diffusivity shifts between these two classes of solvents, as seen in Eq. (15). In Eq. (15), D_A^{0*} is the CO_2 diffusivity and D_B^{0*} is the amine diffusivity both measured experimentally in an aqueous solvent, whereas D_A^0 can be either obtained experimentally or evaluated by the Wilke-Chang correlation.

$$D_B^0 = \left(\frac{D_A^0}{D_A^{0*}}\right) \cdot D_B^{0*} \tag{15}$$

The amine diffusivity also decreases with viscosity, and less controversially so, as both Versteeg and van Swaaij[31] and Snijder et al.[35] have verified in practice that such decrease follows the power of z = 0.6, as expressed in Eq. (16).

$$D_B = D_B^0 \cdot \left(\frac{\eta^0}{\eta}\right)^{0.6} \tag{16}$$

2.3. Chemical kinetics in water-lean solvents

The issue of how reaction kinetics behave in the shift from aqueous to water-lean has been studied since the inception of water-lean solvents, back in the 1980s. For the amines monoethanolamine (MEA), diethanolamine (DEA), ethylenediamine (EDA) and isopropanolamine (MIPA), Sada et al.[18–20] have found a way to correlate the dielectric permittivity of the pure solvents ε with the direct amine-CO_2 reaction kinetic rate constant k_2 and with the ratio between the direct zwitterion-base kinetic rate constant k_b and the reverse amine-CO_2 reaction kinetic rate constant k_{-1}. According to their findings, both k_2 and k_b/k_{-1} generally decrease with a decrease in ε, arguably due to the destabilization of the amine carbamate brought from shifting from aqueous to water-lean. This behavior has been further observed by Park et al. for DEA and MDEA[33,36] and by Hwang et al. for diisopropanolamine[34].

Nevertheless, the nature of this relationship is not entirely clear. Both Sada et al. and Park et al. have proposed that such decrease is typically exponential. However, there are exceptions to this rule. One remarkable exception is the case of MEA. Aqueous MEA 0.5–2 M has a k_2 = 7740 $L \cdot mol^{-1} \cdot s^{-1}$ and $k_b/k_{-1} = \infty$ $L \cdot mol^{-1}$ (meaning that the conversion from zwitterion to

carbamate is infinitely faster than its conversion back to MEA). Meanwhile, in mixtures of MEA 0.5–2 M with methanol, ethanol and 2-propanol, k_2 = 8330 $L \cdot mol^{-1} \cdot s^{-1}$ and k_b/k_{-1} assumes respectively the values of 0.78, 0.35 and 0.27 $L \cdot mol^{-1}$. In other words, while the exponential decrease with ε is observed for k_b/k_{-1}, an actual increase is observed for k_2 – an increase that could perhaps be attributed to the difficulties of fitting both these parameters at the same time to experimental data. Regardless of the reasons, this indicates that the effects of ε on kinetic rate constants should (i) be considered on a case by case basis with regards to each individual amine and (ii) not be taken entirely at face value, but merely as interpolations of available experimental data. Therefore, any extrapolations should be carried with caution.

For the case of 0.5–2 M MEA, the polynomials expressed in Eqs. (17) and (18) have been fitted to data obtained by Sada et al.[19] in water-lean solvents to represent how kinetic rate constants vary with pure diluent dielectric permittivities. These equations are useful for interpolating empirical values, with the caveats that neither is the estimated k_2 constant for all solvents other than water nor does the estimated k_b/k_{-1} go to ∞ in aqueous solvents.

$$ln(k_2)_{MEA} = -2.628 \cdot 10^{-5} \cdot \varepsilon^2 + 1.330 \cdot 10^{-3} \cdot \varepsilon + 9.012 \quad (17)$$

$$ln\left(\frac{k_b}{k_{-1}}\right)_{MEA} = 3.863 \cdot 10^{-3} \cdot \varepsilon^2 - 1.228 \cdot 10^{-1} \cdot \varepsilon - 3.492 \cdot 10^{-1} \quad (18)$$

2.4. Vapor-liquid equilibrium in water-lean solvents

As verified before, substitution of water by an organic diluent shifts the vapor-liquid equilibrium curve towards less CO_2 absorption for a fixed CO_2 partial pressure [10,11,14]. Much like what has been reported for k_2 and k_b/k_{-1}, this is hypothesized to be due to the increased destabilization of the carbamate in water-lean solvents. In a previous study[14], a point was made in that ε alone is not enough to explain this equilibrium shift. The reason for that is that there are several mechanisms for electrolyte stabilization in liquid solvents other than dipole-dipole interactions typically associated with ε – as a matter of fact, the combined actions of van der Waals forces, dipole-dipole forces and hydrogen bonding forces should all be considered when discussing the solvation of carbamate and protonated amine salts.

In the present study, however, a decision was made to take a step back and try to focus on the effects of ε on α versus p_A alone. This comes both from convenience as from necessity. It is convenient because, as shown in Wanderley et al.[14], at least for MEA-based water-lean solvents, the dielectric permittivity of the diluent correlates quite well with the magnitude of the equilibrium shift. This is also consistent with the discussion presented by Fialkov and

Chumak[37] and by Sen et al.[38], who clearly express the shift in equilibrium constants of a reaction as a function of the dielectric permittivity of its diluent. It is necessary because no other practical working correlation has been found in literature or observed so far. Moreover, although many VLE data points for water-lean solvents were obtained in Wanderley et al.[10], most of them referred to loadings very close to or above $\alpha = 0.5$, an interval where the assumption that the only pathways for CO_2 fixation are physical absorption and carbamate formation ceases to have strength.

Therefore, we have borrowed the data reported previously by our group[14] for directly correlating the shift in VLE to the dielectric permittivity ε. Such approach, as it shall be seen, has a great impact on the results obtained in the parametric analysis. To curb this impact, two very clear case studies will be delimitated.

- CASE A – In this scenario, the equilibrium shift happens as reported by Wanderley et al.[14] and its intensity will be represented by Eq. (19) – with the clear admonition that Eq. (19c) has been interpolated only for MEA-based solvents. Eq. (19) shows that, given a function $\alpha^* = f(p_A)$ that describes how α^* varies with p_A in aqueous solvents of a certain amine, the equilibrium shift can be approximated by employing the same function applied to a modified CO_2 partial pressure p_A/ψ.
- CASE B – No equilibrium shift will be considered at all, and the VLE behavior of the water-lean solvent will be set to be the same as that of the aqueous solvent.

$$\alpha^* = f(p_A) \tag{19a}$$

$$\alpha = f\left({}^{p_A}/_{\psi}\right) \tag{19b}$$

$$ln(\psi) = 195.3 \cdot (78.5 - \varepsilon) \tag{19c}$$

These case studies, CASE A and CASE B, are defined in a way such as that the behavior of a real water-lean solvent would be expected to fall inbetween one approach and the other. In a way, they serve to delimit a confidence interval for the conclusions obtained in the course of this research.

For the function $\alpha^* = f(p_A)$, we have employed the soft model fitted by Aronu et al.[39] that represents how CO_2 partial pressure varies as a function of loading for aqueous 30 %wt. MEA solutions. This soft model equation has to be inverted numerically so that loading is given as a function of CO_2 partial pressure.

2.5. Electrostatic phenomena and salting-out

Absorption of CO_2 and its consequent reaction with amine forms electrolytic species which are responsible for a myriad of electrostatic phenomena in the solvent. Among them, the two most remarkable to the capture process are the increase in viscosity and the decrease in CO_2 physical solubility, both caused by mounting intermolecular forces and associated reduction of intermolecular space.

The decrease in gas solubility due to electrolyte formation is typically called *salting-out*. This phenomenon in the context of CO_2 capture has been well discussed by Browning and Weiland[40], who also offer a quantification of this effect. To do so, they employ the modified Sechenov correlation (also known as van Krevelen correlation) shown in Eq. (20).

$$\ln\left(\frac{H_A}{H_A^*}\right) = h \cdot I \tag{20a}$$

$$I = \frac{1}{2} \cdot \sum C_i \cdot {Z_i}^2 \tag{20b}$$

$$h = h_+ + h_- + h_g \tag{20c}$$

In Eq. (21), one can see how the creation of electrolytes affect the CO_2 Henry's coefficient in the liquid. The parameter I defined in Eq. (20b) is called the ionic strength. Since the only reaction being considered in this study is carbamate formation, Eq. (20b) can be reduced by observing that carbamate and protonated amine shall have the same concentration $C_C = C_D$ and electrical charges of $Z_C = -1$ and $Z_D = +1$ respectively – and therefore $I = C_C$ as well. The parameters expressed in Eq. (20c) are the van Krevelen modifiers, which are specific for each cation (h_+), anion (h_-) and gas (h_g). For CO_2, $h_g = -0.019$ L·mol^{-1}. The remainder two parameters are specific to each amine, and Browning and Weiland[40] have helpfully regressed their values for MEA and DEA electrolytes. In MEA, $h_+ = 0.055$ L·mol^{-1} and $h_- = 0.054$ L·mol^{-1}. With these values, the van Krevelen modifier h calculated by Eq. (20c) will be clearly positive, and Eq. (20a) shows that the Henry's coefficient H_A for the loaded solution will be higher than that of the unloaded solvent H_A^*, signifying a clear reduction in CO_2 solubility.

One noticeable aspect of Eq. (20) is how it does not depend on the nature of the solvent itself. However, in a previous work[11], it was stipulated that the salting-out effect would be more noticeable in water-lean than in aqueous solutions. The results of that study were unfortunately inconclusive to this aspect. In the meantime, Yuan and Rochelle[9] managed to measure CO_2 solubility in various water-lean solvents containing MEA, NMP and water at two different

loadings ($\alpha = 0.37$ and $\alpha = 0.45$). In aqueous MEA 7 m, a decrease of 6.4 % in CO_2 solubility was observed from lean to rich solvent, whereas it jumped to 7.7 %, 6.9 % and impressive 52 % in semi-aqueous solvents with respectively 1:3, 3:1 and 19:1 NMP-to-water mass ratios. And yet, in this study it has been decided to fix the salting-out in water-lean solvents proportionally equal to that in aqueous solvents. This is not only convenient, but it has been assessed that the salting-out effect has relatively low impact in the calculation of mass transfer rate coefficients. Therefore, rather than trying to fix the Sechenov equation by figuring out a new correlation, we have decided to consider the salting-out effect a source of uncertainty that may slightly favor water-lean solvents in the parametric analysis.

On the other hand, misjudging the influence that shifting the diluent has on how the viscosity η mounts with increased loadings would disproportionally favor water-lean solvents. As shown previously[9,10], η increases more steeply in these solvents than in aqueous solutions. Referring back to Eqs. (14) and (16), one can clearly see how this phenomenon will reduce both diffusivities D_A and D_B, and consequentially the vapor-to-liquid mass transfer coefficients as well. One could consider the following example from Wanderley et al.[10]. In aqueous 30 %wt. MEA, for each extra 0.10 of CO_2 loading the viscosity increases by about 10 %. In NMP or THFA + 30 %wt. MEA, this increase is of almost 60 %. A quick analysis of Eq. (14) shows that this means a reduction of about 6.6–7.3 % in D_A for the aqueous solution whereas in the water-lean solvent this reduction is of about 29–31 % (depending on $z = 0.72$ or $z = 0.8$ as discussed previously). Not only that, but even unloaded water-lean solvents are generally more viscous than aqueous solvents themselves. Increased viscosities upon loadings in water-lean solvents have also been observed by other authors[9,41], all of which paint a similar picture. Clearly, the viscosity issues of this class of absorbents cannot be ignored.

This study has tried to correlate the increase in viscosity in water-lean solvents to the dielectric permittivity of the diluent ε. This is a natural approach considering everything that has been discussed previously: the electrostatic properties of the solution are not only responsible for kinetic and equilibrium effects on the reaction between CO_2 and amine, but also for the solvent-solute interactions which define viscosity variations. And fortunately, this is also completely consistent with the theoretical and mathematical explanation given in Esteves et al.[42] regarding how the dielectric permittivity of the milieu affects the viscosity of electrolyte solutions. Since ε is already being used in Eqs. (17)–(19) to describe those phenomena, it will be used henceforth to describe the latter as well.

2.6. Exemplifying the parametric analysis approach

The simplest way to approach the analysis introduced in this work is by considering the case of absorption in an unloaded solvent put in contact with an atmosphere of pure CO_2. To do so, one can focus initially on water-lean solvents which have been previously evaluated in the literature.

Table 1 shows the relevant parameters for a number of aqueous and water-lean solvents. It is important to highlight that many of these parameters were not actually measured in the corresponding references. Consider for example the case of Hwang et al.[34], who have gathered data for mixtures of DIPA and various organic diluents. Although they report the Henry's coefficient of CO_2 in water-lean solvents, what they did was measure the CO_2 solubility in a pure organic diluent, such as ethanol, and then assumed that the CO_2 solubility in ethanol + DIPA would be exactly the same. Meanwhile, D_A and D_B were both evaluated by the Wilke-Chang correlation. In that light, one could argue that the parameters actually measured by Hwang et al.[34] were k_2 and k_b/k_{-1}, and both of these are subject to the assumptions that D_A, D_B and H_A really hold – since their experimental procedure revealed overall mass transfer coefficients, not the kinetic constants themselves. And yet, Table 1 includes the best published data on the kinetics of amines in water-lean solvents, so that any serious discussion on the mass transfer phenomena in this class of absorbents often relies in this information.

Table 1. Parameter for aqueous and water-lean solvents compiled from literature.

*Values were not disclosed in Sada et al.[19], but estimated by us through retroactively applying the same approach used by Park et al.[33,36] and Hwang et al.[34] discussed in this section.

Diluent	Amine	C_B^0	T	k_2	k_b/k_{-1}	D_A	D_B	H_A	Ref.
H2O	MEA	0.5–2.0	303	7740	∞				[19]
MeOH	MEA	0.5–2.0	303	8330	0.78				[19]
EtOH	MEA	0.5–2.0	303	8330	0.35				[19]
2-PrOH	MEA	0.5–2.0	303	8330	0.27				[19]
H2O	DEA	0.5–1.5	303	1100	1.20	1.950*	0.667*	2.895*	[19]
MeOH	DEA	0.5–1.5	303	340	1.00	8.370*	1.721*	0.637*	[19]
EtOH	DEA	0.5–1.5	303	290	0.71	3.880*	0.912*	0.811*	[19]
2-PrOH	DEA	0.5–1.5	303	240	0.77	2.730*	0.482*	1.055*	[19]
n-ButOH	DEA	1.0–3.0	298	187	0.85	0.876	0.398	1.089	[33]

MEG	DEA	1.0–3.0	298	340	0.97	0.121	0.055	3.753	[33]
MPG	DEA	1.0–3.0	298	230	0.90	0.054	0.025	0.409	[33]
PC	DEA	1.0–3.0	298	280	0.92	1.077	0.489	0.798	[33]
H2O	MIPA	0.5–1.5	303	5920	∞				[18]
MeOH	MIPA	0.5–1.5	303	4390	0.94				[18]
EtOH	MIPA	0.5–1.5	303	3640	0.53				[18]
2-PrOH	MIPA	0.5–1.5	303	3270	0.31				[18]
H2O	DIPA	1.0–3.0	298	583	0.17	1.950	0.724	2.895	[34]
MeOH	DIPA	1.0–3.0	298	76	0.46	8.370	1.784	0.637	[34]
EtOH	DIPA	1.0–3.0	298	47	0.62	3.880	0.946	0.811	[34]
2-PrOH	DIPA	1.0–3.0	298	36	0.66	2.730	0.499	1.055	[34]
n-ButOH	DIPA	1.0–3.0	298	35	0.77	0.876	0.413	1.089	[34]
MEG	DIPA	1.0–3.0	298	75	0.42	0.121	0.057	3.753	[34]
MPG	DIPA	1.0–3.0	298	47	0.52	0.054	0.025	0.409	[34]
PC	DIPA	1.0–3.0	298	54	0.58	1.077	0.507	0.798	[34]

Where C_B^0 s in mol·L^{-1}, T is in K, k_2 is in L·mol^{-1}·s^{-1}, k_b/k_{-1} is in L·mol^{-1}, D_A and D_B are in 10^9 m^2·s^{-1} and H_A is in bar·L·mol^{-1}.

With the parameters shown in Table 1, one can start analyzing the absorption behavior of CO_2 in both aqueous and water-lean solvents. In an unloaded solution, the reaction will be far from reaching equilibrium and K can be set to a very high value ($K \approx \infty$). For loaded solutions, we have regressed K from the vapor-liquid equilibrium of CO_2 in aqueous solutions of DEA from the datapoints obtained by Lee et al.[43], and then updated K in water-lean solvents by employing the dielectric permittivity ε of the pure diluents and Eq. (19). Notice that Eq. (19) was fitted for MEA data and one would have to be extremely cautions before extending it to DEA. Fortunately, this is not relevant when dealing with unloaded solutions, or essentially any solution far from equilibrium loading.

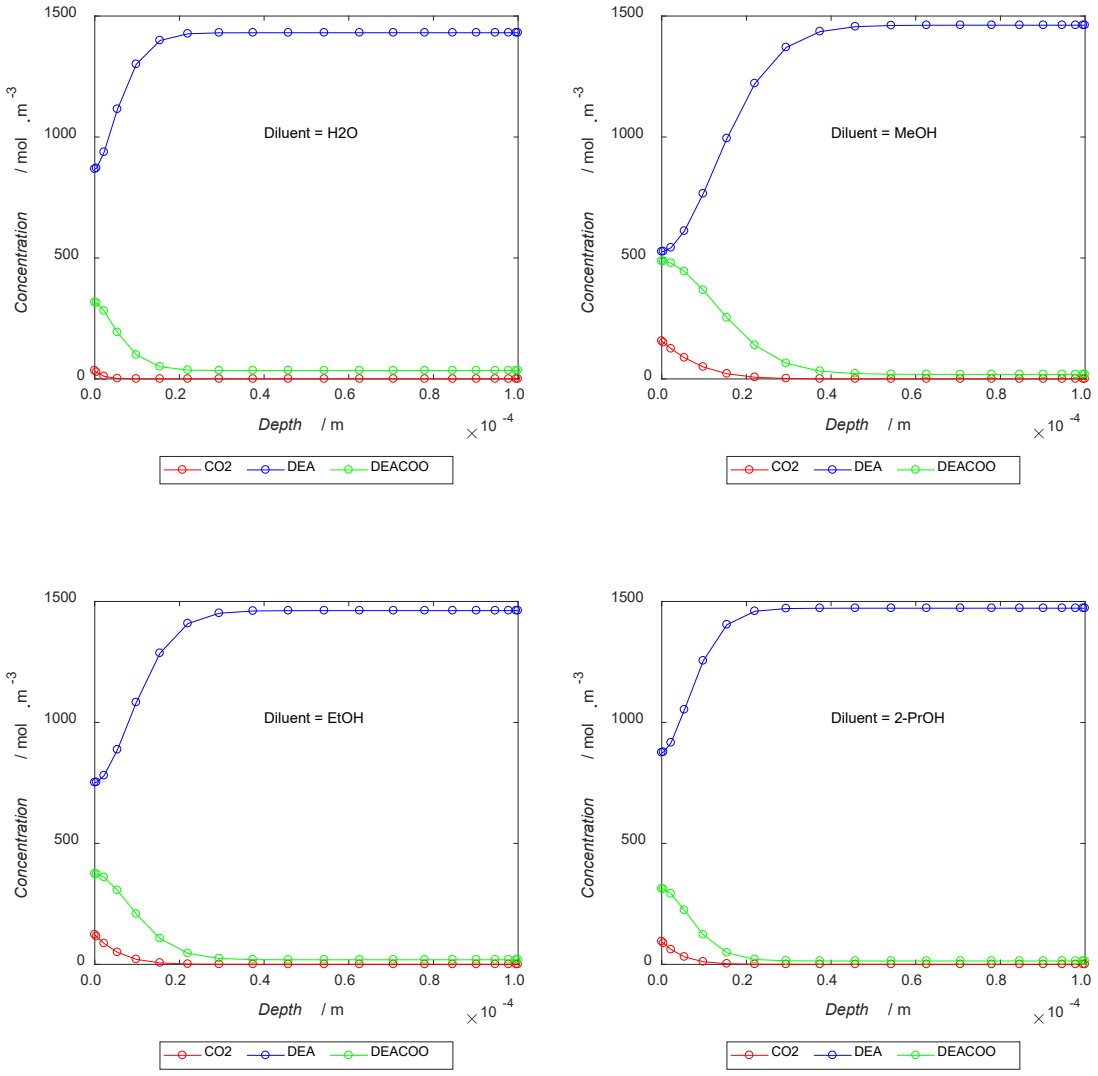

Figure 1. Predicted penetration profiles for unloaded solvents with 1.5 M DEA in contact with CO_2 partial pressure $p_A = 10^5$ Pa of CO_2 for a surface renewal time $\tau \approx 0.05$ s. Solvents = water (H2O), methanol (MeOH), ethanol (EtOH) and 2-propanol (2-PrOH).

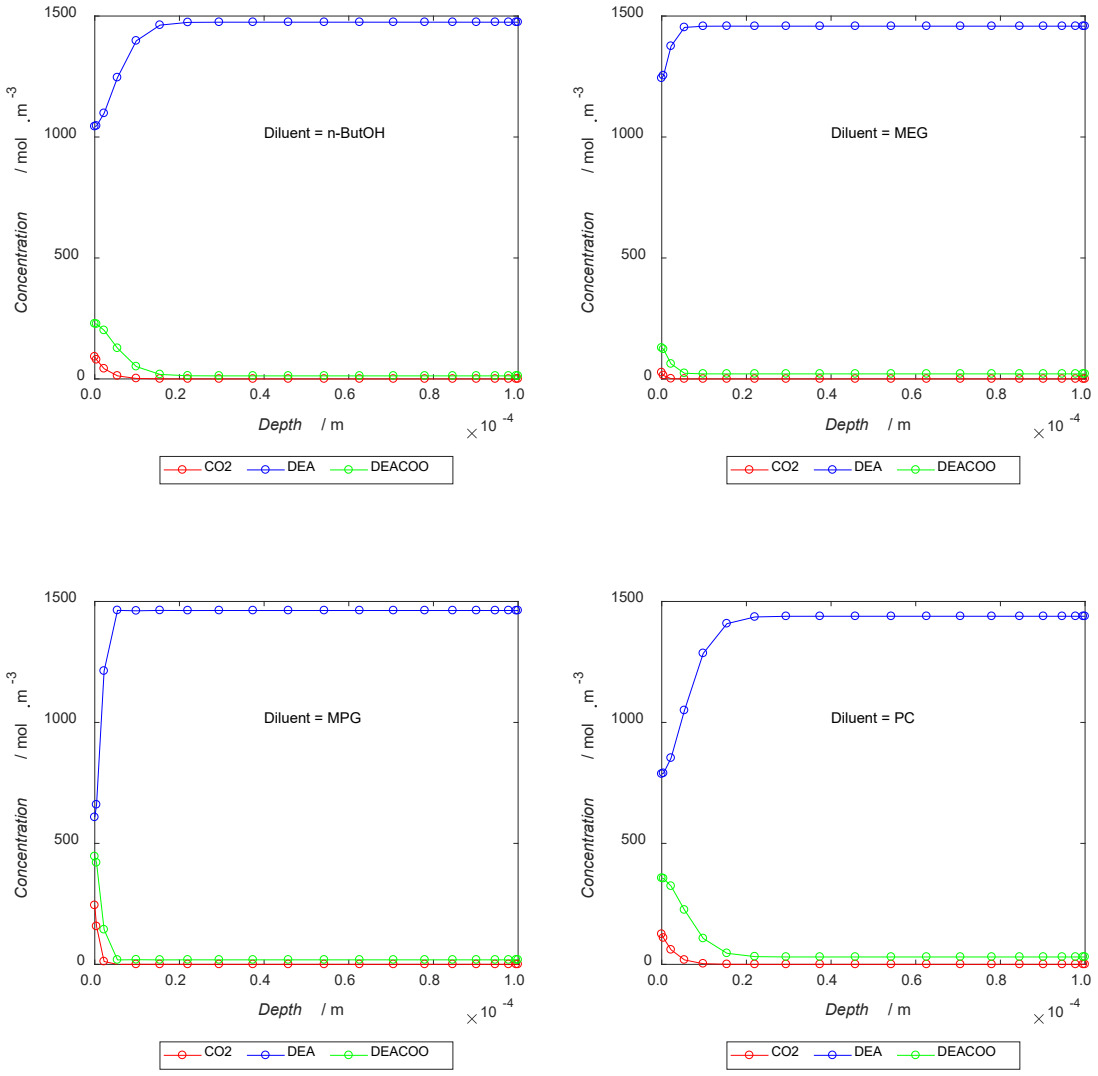

Figure 2. Predicted penetration profiles for unloaded solvents with 1.5 M DEA in contact with CO_2 partial pressure $p_A = 10^5$ Pa of CO_2 for a surface renewal time $\tau \approx 0.05$ s. Solvents = n-butanol (n-ButOH), ethylene glycol (MEG), propylene glycol (MPG) and propylene carbonate (PG).

One can now analyze Figure 1 and Figure 2 together with Table 1 to investigate the effects that some parameters have on the absorption performance of the solvents. The first profile in Figure 1 is that of aqueous 1.5 M DEA. Following that, a series of alcohols is accounted for, from 1 to 4 carbons long (methanol, ethanol and 2-propanol in Figure 1 to n-butanol in Figure 2). The behavior of the penetration profile following this series is evident. As the carbon chain gets longer, the viscosity of the alcohol increases, and consequentially the diffusivities of both CO_2 and amine decrease. Meanwhile, CO_2 solubility also decreases. The dielectric permittivity goes

down, dragging together the kinetic coefficients k_2 and k_b/k_{-1}. Altogether these effects have three consequences in the profiles: (i) the CO_2 physical absorption decreases from methanol to n-butanol, as evidenced by the red-dotted-lines showing lower concentrations of molecular CO_2; (ii) the amount of DEA that reacts with CO_2 in that limited timespan also decreases, seen in the green-dotted-lines showing lower concentrations of carbamate; (iii) the penetration depth is reduced, and the point in space in which all curves reach their equilibrium values clearly diminishes from methanol to n-butanol. Ethylene glycol + DEA is an extreme example of this behavior, having very high viscosity and very low CO_2 solubility. Propylene glycol has high CO_2 solubility, but high viscosity as well, and its penetration depth is the lowest of all solvents in both Figure 1 and Figure 2. For these reasons, these are the two diluents with worst performance of all the ones considered for DEA-based water-lean solvents. Finally, propylene carbonate is able to couple high CO_2 solubility with moderate viscosity and kinetic coefficients, producing a profile similar to that of ethanol while having the big advantage of being comparatively non-volatile.

This analysis suggests that it is possible to, given a base case, comparatively evaluate the effects of shifting diffusivities, kinetic coefficients and solubility on the overall performance of the solvent. By overall performance, we mean the liquid phase mass transfer coefficient for CO_2 capture. This coefficient k_g^* is defined as by Eq. (21a). What this expression shows is that k_g^* is the change in CO_2 concentration C_A plus the change in carbamate concentration C_C evaluated over the total penetration depth at an instant τ (the surface renewal time), divided by τ itself and by the change in CO_2 partial pressure p_A that drives the absorption. Therefore, it is a measure of how fast the vapor-to-liquid mass transfer proceeds over a unitary increase in driving force. For comparison, Eq. (21b) provides an equivalent expression to define k_g^*, wherein it becomes explicit that this mass transfer coefficient accounts for the rate of CO_2 absorption into the liquid set in motion by a differential CO_2 partial pressure between the interface and the liquid bulk. Furthermore, k_g^* is merely a measure of liquid phase mass transfer coefficient, with no regards to gas phase mass transfer phenomena whatsoever.

$$k_g^* = \frac{\int_0^\infty \{C_A(\tau, x) - C_{A,i} + C_C(\tau, x) - C_{C,i}\} \cdot dx}{(p_A - p_{A,i}) \cdot \tau} \tag{21a}$$

$$k_g^* = \frac{\Delta C_A}{\Delta p_A \cdot \tau} = \frac{N_A}{\Delta p_A} \tag{21b}$$

The k_g* is going to be the parameter used to evaluate variations in solvent performance caused by shifting solvent properties. Following the DEA 1.5 M example, Table 2 shows how the mass transfer coefficients change in a series of diluents. It summarizes the results presented in Figure 1 and Figure 2 and makes it more evident that some solvents may have a net positive effect on CO_2 absorption when compared to water, while others do not.

Table 2. Comparison between mass transfer coefficients in solvents based on DEA 1.5 M (unloaded, $p_A = 10^5$ Pa, $\tau = 0.05$ s)

Diluent	k_g* / mol·m^{-3}·Pa^{-1}·s^{-1}	k_g* increment
H2O	$4.26 \cdot 10^{-7}$	0 %
MeOH	$1.87 \cdot 10^{-6}$	+338 %
EtOH	$9.88 \cdot 10^{-7}$	+132 %
2-PrOH	$6.39 \cdot 10^{-7}$	+50 %
n-ButOH	$3.44 \cdot 10^{-7}$	−19 %
MEG	$5.53 \cdot 10^{-8}$	−87 %
MPG	$2.23 \cdot 10^{-7}$	−48 %
PC	$5.62 \cdot 10^{-7}$	+32 %

However interesting this preliminary analysis may be, it is also very limited. For practical purposes, CO_2 absorption in the industry does not rely on unloaded lean solvents, neither does it involve driving forces as high as 10^5 Pa. On the contrary, the lean solvent in the absorber operates in a range of loadings and of driving forces $\Delta p_A = p_A - p_{A,i}$ which ideally are as small as possible.

Therefore, we have designed a study in which Δp_A is constant ($\Delta p_A = 100$ Pa) and CO_2 partial pressure in the absorber varies from 110–2610 Pa. The loadings of the lean solvent before mass transfer are defined by p_A and Δp_A, so that the vapor with partial pressure $p_A = 110$ Pa is in contact with the lean amine which has equilibrium partial pressure $p_{A,i} = 10$ Pa. Thus, the driving force is constant and kept relatively small throughout the column, and k_g* will vary accordingly together with the solvent loading. This can be seen on Figure 3.

What is remarkable in Figure 3 is how quickly the loading increases with increasing CO_2 partial pressure, and therefore how fast the mass transfer coefficient k_g* drops as the lean solvent flows down the absorber. This is due to all of the electrostatic phenomena mentioned in previous sections – in first place the increase in viscosity and decrease in diffusivities, in second

place the salting-out of CO_2. Figure 3 however serves merely an illustrative purpose, as the increase of viscosity with loading in aqueous DEA was estimated to be the same as the one observed for aqueous MEA. The salting-out parameters for DEA were obtained in Browning and Weiland[40], and the vapor-liquid equilibrium is adapted from Lee et al.[43]. The average k_g* measured throughout the column is $k_g^* = 1.19 \cdot 10^{-7}$ mol·m^{-3}·Pa^{-1}·s^{-1}, substantially smaller than $k_g^* = 4.26 \cdot 10^{-7}$ mol·m^{-3}·Pa^{-1}·s^{-1} for unloaded aqueous 1.5 M DEA seen on Table 2. By average k_g*, we refer to the geometric average of the k_g*s evaluated at each pressure in the evaluated span (in the present case, from p_A = 110–2610 Pa) taken at linearly divided intervals.

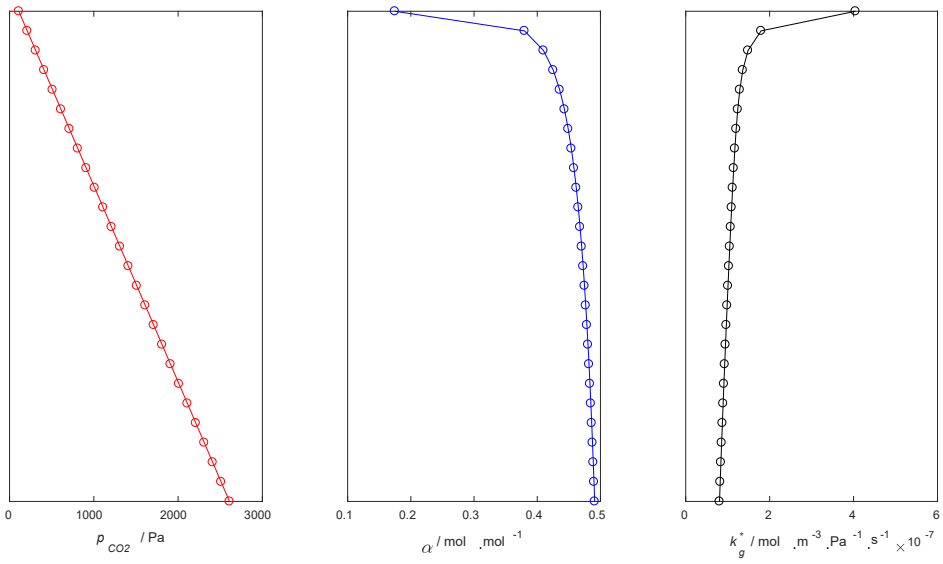

Figure 3. CO_2 partial pressure, loading and mass transfer coefficient profiles in a column operating with aqueous 1.5 M DEA.

2.7. Analysis of hypothetical water-lean solvents based on 30 %wt. MEA

As discussed previously, the properties of hypothetical water-lean solvents can be calculated by using parameters such as molar mass, density and viscosity (for the Wilke-Chang correlation), Henry's coefficient and dielectric diffusivity. A compilation of these properties for this set of solvents can be found in Appendix 1. The Wilke-Chang correlation is applied to the whole solvent, i.e. considering individually the properties of the pure diluent plus the properties of MEA and treating them with a mixing rule. The Henry's coefficient of CO_2 in the solvent is also calculated with a mixing rule. The rules we have employed in this study can be found in Appendix 2.

We have calculated the average mass transfer coefficient k_g^* for a set of hypothetical water-lean solvents based on 30 %wt. MEA considering CO_2 absorption in a column where p_A in equilibrium with the loaded solvent varies between 0–1000 Pa, Δp_A = 100 Pa and τ = 0.05 s. The enhancement of k_g^* when compared to aqueous 30 %wt. MEA is shown in Table 3 for CASE A. Figure 4 shows the mass transfer coefficient profiles obtained for the CASE A analyses as a function of the CO_2 partial pressure in the column.

Table 3. Comparison between mass transfer coefficients in hypothetical solvents based on 30 %wt. MEA (p_A = 0–1000 Pa, Δp_A = 100 Pa, τ = 0.05 s).

Name	k_g^* evaluated at p_A = 500 Pa	k_g^* averaged from p_A = 0–1000 Pa
acetone	$1.09 \cdot 10^{-6}$	$1.62 \cdot 10^{-6}$
benzaldehyde	$7.17 \cdot 10^{-7}$	$1.04 \cdot 10^{-6}$
butanol	$4.89 \cdot 10^{-7}$	$6.97 \cdot 10^{-7}$
2-butanol	$4.29 \cdot 10^{-7}$	$6.13 \cdot 10^{-7}$
t-butanol	$4.05 \cdot 10^{-7}$	$5.84 \cdot 10^{-7}$
cycloheptanone	$6.06 \cdot 10^{-7}$	$8.92 \cdot 10^{-7}$
cyclohexanol	$2.56 \cdot 10^{-7}$	$3.52 \cdot 10^{-7}$
cyclohexanone	$6.30 \cdot 10^{-7}$	$9.14 \cdot 10^{-7}$
cyclopentanone	$7.00 \cdot 10^{-7}$	$1.04 \cdot 10^{-6}$
dimethyl sulfoxide	$1.07 \cdot 10^{-6}$	$1.27 \cdot 10^{-6}$
dimethyl formamide	$1.28 \cdot 10^{-6}$	$1.61 \cdot 10^{-6}$
ethanol	$7.77 \cdot 10^{-7}$	$1.07 \cdot 10^{-6}$
ethylene chloride	$7.96 \cdot 10^{-7}$	$1.22 \cdot 10^{-6}$
ethylene glycol	$2.99 \cdot 10^{-7}$	$3.51 \cdot 10^{-7}$
N-formyl morpholine	$5.06 \cdot 10^{-7}$	$7.12 \cdot 10^{-7}$
glycerol	$8.84 \cdot 10^{-9}$	$1.01 \cdot 10^{-8}$
heptanol	$4.50 \cdot 10^{-7}$	$6.54 \cdot 10^{-7}$
hexanol	$4.62 \cdot 10^{-7}$	$6.70 \cdot 10^{-7}$
isoamyl alcohol	$4.32 \cdot 10^{-7}$	$6.28 \cdot 10^{-7}$
isobutanol	$4.40 \cdot 10^{-7}$	$6.26 \cdot 10^{-7}$
isopropanol	$5.14 \cdot 10^{-7}$	$7.25 \cdot 10^{-7}$
methanol	$1.27 \cdot 10^{-6}$	$1.67 \cdot 10^{-6}$

methyl ethyl ketone	$9.85 \cdot 10^{-7}$	$1.47 \cdot 10^{-6}$
nitrobenzene	$9.60 \cdot 10^{-7}$	$1.20 \cdot 10^{-6}$
N-methyl-2-pyrrolidone	$1.09 \cdot 10^{-6}$	$1.40 \cdot 10^{-6}$
pentanol	$4.42 \cdot 10^{-7}$	$6.37 \cdot 10^{-7}$
phenyl acetonitrile	$5.98 \cdot 10^{-7}$	$8.57 \cdot 10^{-7}$
propanol	$5.59 \cdot 10^{-7}$	$7.81 \cdot 10^{-7}$
propionitrile	$1.29 \cdot 10^{-6}$	$1.74 \cdot 10^{-6}$
propylene carbonate	$1.24 \cdot 10^{-6}$	$1.43 \cdot 10^{-6}$
pyridine	$7.04 \cdot 10^{-7}$	$1.05 \cdot 10^{-6}$
sulfolane	$7.29 \cdot 10^{-7}$	$8.60 \cdot 10^{-7}$
water	$9.23 \cdot 10^{-7}$	$1.06 \cdot 10^{-6}$

In Table 3, two distinct classes of results can be observed. The first class is that of water-lean solvents that would not deliver enhanced mass transfer rates when compared to aqueous solvents. This comprises any alcohol heavier than methanol, plus some diluents such as ethylene glycol, N-formyl morpholine and sulfolane. It is interesting to stress these latter three because they are often considered promising components for water-lean solvent formulation. As it turns out, even though N-formyl morpholine and sulfolane are both good physical solvents for CO_2 absorption, their high viscosity results in that one could hardly expect the mass transfer rates in mixtures between these chemicals and 30 %wt. MEA to increase due to enhanced CO_2 solubility. A second class of solvents can hypothetically deliver enhanced mass transfer rates. This class includes methanol, acetone, N-methyl-pyrrolidone and propylene carbonate.

Figure 4 shows the mass transfer coefficient profiles for some of the hypothetical solvents calculated using the CASE A analysis. These solvents are divided into series of alcohols, ketones and miscellaneous organic diluents. Some interesting facts can be observed in our results. Firstly, it is remarkable that the best performing organic diluents tend to be very volatile compounds (methanol, ethanol, acetone, methyl ethyl ketone). This is due to these solvents usually having very low viscosity. There is no clear relationship in literature between viscosity and volatility, but it can be argued that these two parameters are somehow connected by electrostatic phenomena. Viscosity is an important parameter, being fundamental in explaining the results for the miscellaneous organic compounds seen on the bottom part of Figure 4. This series of solvents offer good alternatives in case one is interested in diluents with low volatility

for reducing reboiler duties (see Section 4), though they are more susceptible to loss in CO_2 capture capacity due to thermal phenomena in the absorber (see Section 3).

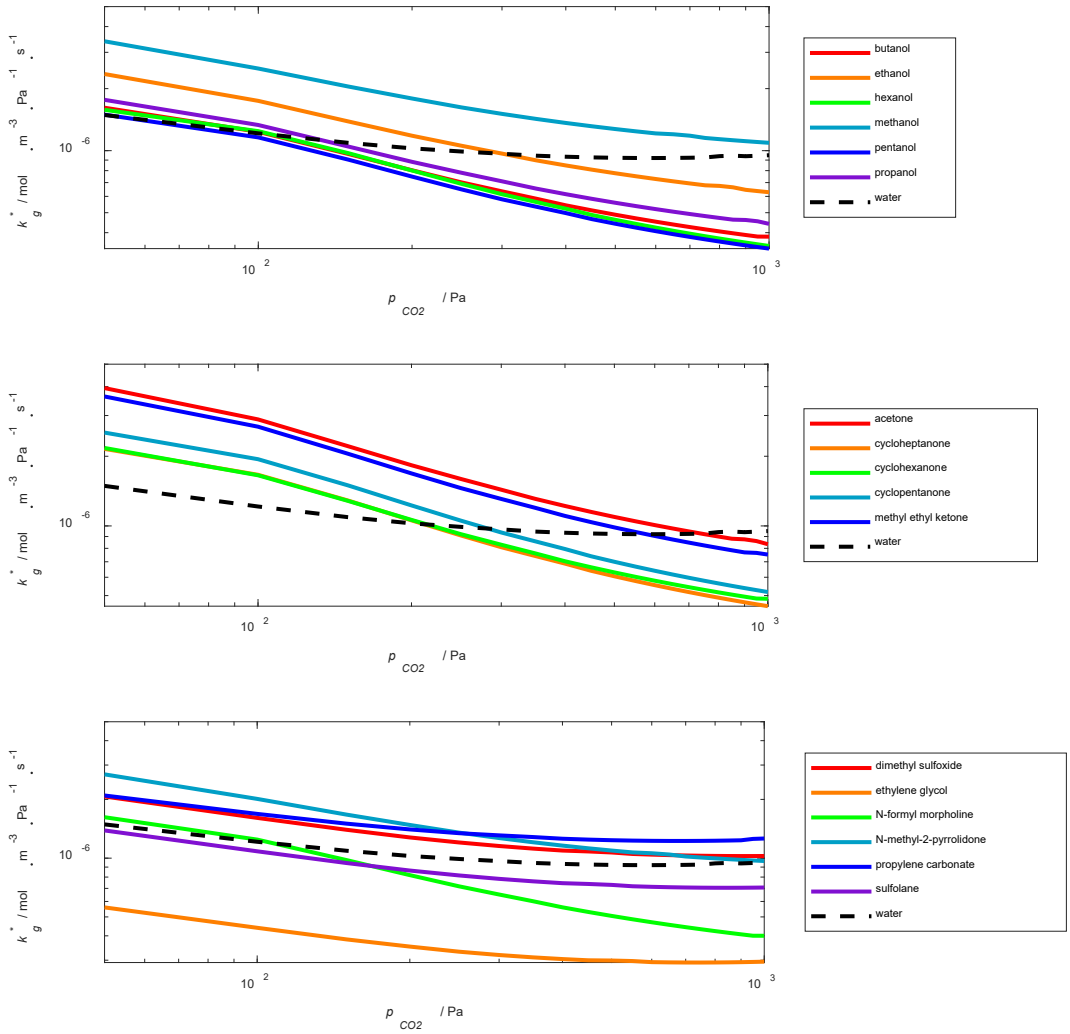

Figure 4. Mass transfer coefficient profiles in terms of equilibrium CO_2 partial pressure for water-lean solvents based on 30 %wt. MEA plus series of alcohols, ketones and miscellaneous organic diluents (p_A = 0–1000 Pa, Δp_A = 100 Pa, τ = 0.05 s). Results obtained for CASE A type analyses.

Finally, it is important to mention that, although Figure 4 shows k_g^* in terms of CO_2 partial pressures in the column, the fact that all organic solvents analyzed have lower ε than water implies that no hypothetical water-lean solvent formulation with 30 %wt. MEA will achieve a rich loading as high as that of the aqueous solvent. To illustrate this, Figure 5 shows the mass

transfer coefficient profiles for the miscellaneous series of organic diluents as a function of CO_2 loading. Due to their low dielectric permittivity, the decrease in mass transfer coefficients with loading observed even for promising alternatives such as N-methyl-2-pyrrolidone and propylene carbonate is steeper in water-lean solvents than in aqueous amines.

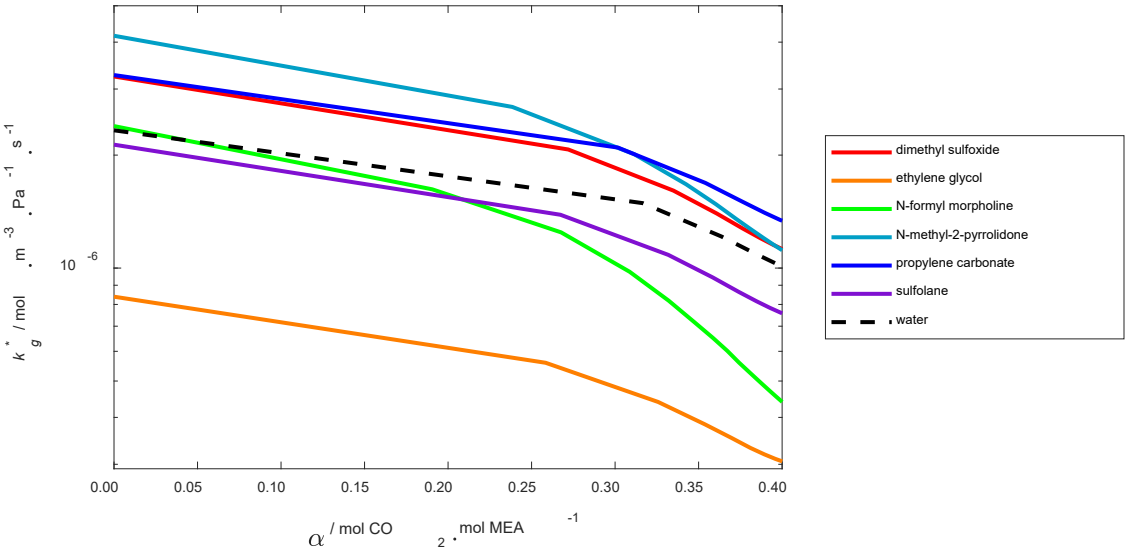

Figure 5. Mass transfer coefficient profiles in terms of CO_2 loading for water-lean solvents based on 30 %wt. MEA plus a series of miscellaneous organic diluents (p_A = 0–1000 Pa, Δp_A = 100 Pa, τ = 0.05 s). Results obtained for CASE A type analyses.

The behaviors observed in Figure 5 are strikingly similar to the ones obtained experimentally by Yuan and Rochelle[9,44] and by Wanderley et al.[14]. Other than these studies, no other publications were found dealing with the mass transfer rates in loaded water-lean solvents, making any comparison with literature data the more complicated. Moreover, comparisons with the data from Wanderley et al.[14] are difficult because of the particularities of some of these solvents that go beyond this parametric analysis (e.g. sulfolane plus MEA presents phase separation upon CO_2 absorption[45], NMP possibly reacts with CO_2 directly[46]). Nevertheless, the trends resulting from our simulations are indicative that their approach is correct.

The decrease in maximum attainable rich loading in water-lean solvents is a fact that is important to keep in mind. Because of that, the only alternative for operating the amine scrubber with the same amount of solvent used in the aqueous process is by similarly reducing the lean loadings. As it shall be discussed in Section 4.3, this is equally problematic.

Our approach also enables the calculation of mass transfer coefficients for water-lean solvents containing mixtures of water and organic diluents. Figure 6 shows how the k_g* of a sulfolane-based water-lean solvent with 30 %wt. MEA would vary with the addition of water to the diluent according to our simulation results. Though the profile shown in Figure 6 has a clear inflection, its maximum does not stray too far away from the mass transfer coefficients of either aqueous or non-aqueous 30 %wt. MEA individually. In theory, therefore, this allows the possibility of preparing water-lean solvents with specific proportions of water so as to tune for a better overall performance in the CO_2 capture cycle.

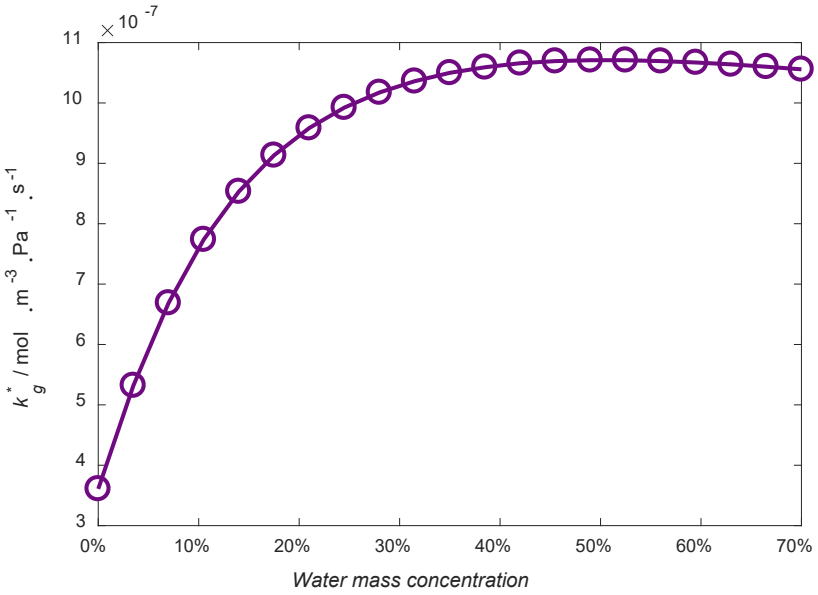

Figure 6. Average mass transfer coefficients calculated for diluents based on mixtures of sulfolane and water plus MEA 30 %wt (p_A = 0–1000 Pa, Δp_A = 100 Pa, τ = 0.05 s). Results for CASE A type analyses.

A parametric analysis of which variables most influence k_g* of different solvents in shown in the Supporting Information material. The takeaway of that study is that the most important parameters are CO_2 diffusivity and solubility, with dielectric permittivity being a relevant secondary parameter if CASE B is considered – but less so in CASE A studies. This is an unsurprising result, and suggests that we can condense our parameter investigation into three main variables: CO_2 solubility, viscosity and dielectric permittivity. This investigation is carried out in the following Section 2.8.

2.8. Viscosity and CO_2 solubility in hypothetical water-lean solvents

Let us imagine that a researcher wants to choose a suitable candidate to prepare a water-lean solvent containing 30 %wt. MEA, possessing only a table with the viscosity of each diluent and its CO_2 physical solubility at typical absorber temperatures. One is interested mainly in obtaining an enhancement of mass transfer rates with the new solvent, i.e. the water-lean solvent resulting of this mixture should deliver higher mass transfer rates than aqueous MEA, otherwise there is no good reason for the shift. As a researcher, one knows that there is a trade-off between viscosity and CO_2 solubility. But how strong is the nature of this trade-off?

Figure 7 addresses this issue with the results of the model developed throughout Section 2. The lines in Figure 7 designate values of η and H_A for which a solvent of fixed ε, varying between $\varepsilon = 20$ and 60, can deliver the same mass transfer coefficient as aqueous MEA. For these calculations, the diffusivities D_A had to be evaluated with the Wilke-Chang expression (Eq. 13), which is a weak function of the diluent molar weight M. Therefore, we have fixed M = 100 $g \cdot mol^{-1}$, as this value is close to the average of that for most interesting diluent candidates (ethylene glycol, N-methyl-2-pyrrolidone, sulfolane), and $\chi = 1.0$.

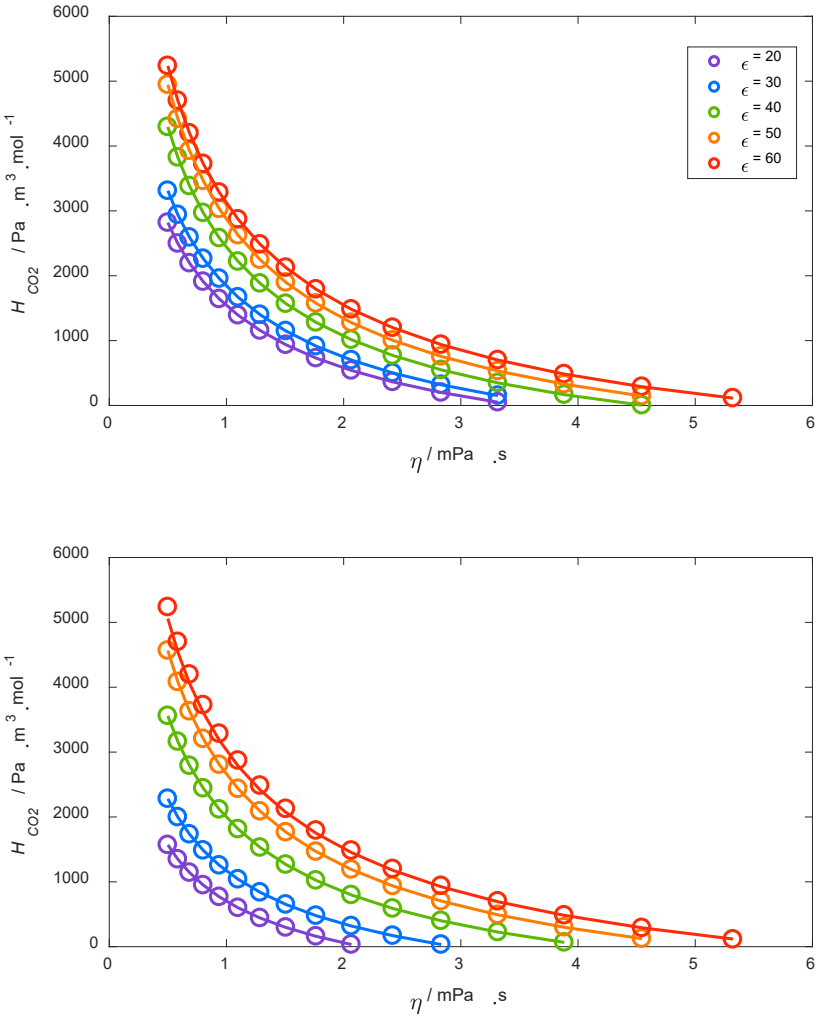

Figure 7. Trade-off between viscosity and Henry's coefficient in water-lean solvents based in 30 %wt. MEA (p_A = 0–1000 Pa, Δp_A = 100 Pa, τ = 0.05 s). The molar weight of the diluent is fixed at M = 100 g·mol^{-1}. Results for CASE A type analyses are in the top, while results for the CASE B type analyses are in the bottom.

To read Figure 7, one must pay notice to the fact that, below each line, the proposed diluent is able to deliver mass transfer coefficients above those of aqueous 30 %wt. MEA. In this sense, it becomes evident that the '*room for maneuver*' is very limited.

In CASE A type analyses, the curves for different dieletric permittivities ε fall very closely by, this being the most optimistic scenario. And still, for diluents above the viscosity of η = 5 mPa·s, there are meager chances of finding corresponding Henry's coefficients low enough so as to make a feasible water-lean solvent. In fact, the corresponding H_A for a valid trade-off

decreases exponentially with η. In other words, the viscosity of a diluent is a lot more impactful than its CO_2 solubility in terms of enhancing mass transfer rates. Meanwhile, CASE B type analyses are even more pessimistic. Due to the viscosity increase with loading, and now unaided by carbamate equilibrium shifts, organic diluents with low ε are barely interesting for solvent formulation. This result reinforces how important the equilibrium shift is to elevate the mass-transfer coefficients of water-lean solvents.

Perhaps a better way of making our point is considering that what is understood as CO_2 solubility is the inverse of the Henry's coefficient as defined in this study. Taking CASE A as an example, Figure 8 shows the trade-off directly in terms of viscosity and CO_2 solubility. This time, the value referring to water is plotted as a black star in the image. Additionally, the data is shown in a semilog plot.

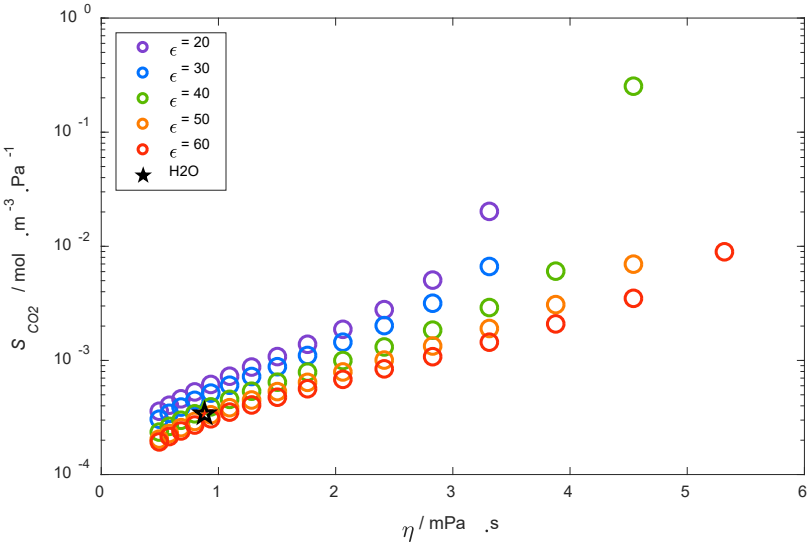

Figure 8. Trade-off between viscosity and CO_2 solubility in water-lean solvents based in 30 %wt. MEA (p_A = 0–1000 Pa, Δp_A = 100 Pa, τ = 0.05 s). The molar weight of the diluent is fixed at M = 100 g·mol^{-1}. Results for CASE A type analyses.

As it can be seen on Figure 8, in solvents a couple of times more viscous than water, the required CO_2 solubility for a valid trade-off is a hundred-fold higher. Though this is not impossible by any means, and while there are solvents that can be found above this theoretical line (N-methyl-pyrrolidone and propylene carbonate being some of them), this puts into perspective the whole enterprise of looking for good physical solvents as primal matter for water-lean solvent formulation. It might be the case that looking for chemicals with lower viscosity could be more interesting than chemicals with high CO_2 solubility.

3. Thermal phenomena in the absorber

In Section 2, it has been assumed that the separation of CO_2 in the absorber column happens at fixed temperature of 25–40 °C. This is not precisely the case in real industrial applications. Even if both the liquid and vapor phases are made to enter the absorber at 40 °C, an array or thermal phenomena will create unique temperature profiles in the column which will depend on several factors, the solvent parameters being but a few of them.

The main parameters evaluated in Section 3 are the diluent heat capacity and its volatility. Organic solvents have mostly always lower heat capacity than water. This means that they have more potential for both heating up due to the exothermic reaction between the amine and CO_2 and cooling down due to heat exchange with the raw gas stream. Meanwhile, the volatility of the diluent has a sensible impact in thermal phenomena, as vaporization of water in the absorber removes heat from the liquid stream and prevents large temperature bulges. When dealing with organic solvents with low saturation pressure, diluent volatilization is depressed and more warming up of the liquid is to be expected. The reverse applies to organic solvents with high saturation pressure. The main consequence of these thermal phenomena is their effect on the equilibrium solubility of CO_2 with the amine – excessive warming up is bound to reduce the solvent capacity for CO_2 capture. Conversely, excessive volatilization of the diluent poses another practical issue, since this vaporized diluent must then be separated and recovered from the clean gas stream.

Many of the issues highlighted in this Section 3 may be countered by efficient design of intercoolers in the absorption column (in case of low-volatility diluents) or solvent recovery mechanisms (in case of high-volatility diluents). These issues have been previously pointed out by Heldebrant et al.[6] and are not unsurmountable, but deserve careful consideration.

The calculation approach adopted in this Section 3 is arguably less sophisticated than the one seen in Section 2. A MESH algorithm[47] relying on mass, energy and chemical equilibrium balances for each tray in a hypothetical absorber column has been employed. This means we have used an equilibrium-based approach instead of the more rigorous rate-based approach. Additionally, though volatility of the diluent has been taken into account, the amine has been deemed completely nonvolatile. These considerations are far from ideal to what concerns rigorous calculations of temperature and concentration profiles, and yet we believe they are sufficient for purely comparative purposes. Furthermore, since we are unable to properly assess the volatility of water in semi-aqueous water-lean solvents, the calculations in Section 3 are

valid only for nonaqueous solvents. Water evaporation in semi-aqueous solvents could result in smoother thermal phenomena in the absorber column, but we have no way of evaluating it in this work.

For the calculations presented in Section 3, the inert component in the raw gas mixtures has been fixed as being methane. A large span of CO_2 concentrations is typically observed in biogas streams[48], having a clear impact on thermal phenomena in the absorber, and thus it is interesting to bring the present discussion closer to the realm of biogas upgrading. However, we might as well have chosen nitrogen or any other inert for this analysis. The properties of the inert gas, given that its solubility in the solvent is negligible, are not very important for our calculations.

For a deeper understanding of the thermal aspects of CO_2 absorption in a column, we refer to Kvamsdal and Rochelle[49]. What follows in Sections 3.1 and 3.2 is a quick summary of the modelling employed in this study, whereas Section 3.3 will apply our analysis for a number of known candidates for water-lean solvent formulation.

3.1. Modelling an isobaric absorber column for evaluating water-lean solvents

For this study, we have assumed that the volatilization of the amine (typically very little compared to that of the diluent) has no impact on the thermal phenomena, so that only CO_2 and diluent are allowed to make the transition between liquid and vapor phases. Meanwhile, all amine remains in the liquid phase, and all gases other than CO_2 (e.g. methane) remain in the gas phase. With that in mind, we have designed a simple MESH algorithm[47] for solving the mass and energy flows in a column with complete thermodynamical equilibrium, wherein the CO_2 partition coefficient is calculated by the soft model parametrized by Aronu et al.[39] for aqueous 30 %wt. MEA and that of the diluent is calculated by Raoult's law with the proper saturation pressures evaluated by Antoine's expression as shown in Appendix 1. All of these are temperature-dependent.

The molar flow rates of CO_2 and diluent in each stage i of the absorber can be expressed respectively by Eqs. (22) and (23).

$$l_A^{i-1} + v_A^{i+1} = l_A^i + v_A^i \tag{22}$$

$$l_{dil}^{i-1} + v_{dil}^{i+1} = l_{dil}^i + v_{dil}^i \tag{23}$$

The total molar flow rates of the liquid and vapor phases is given by Eqs. (24) and (25), which rely on the assumptions that the amine will not be volatilized into the vapor phase and that the inert gas will not be absorbed by the solvent at any significative fraction.

$$l^i = l_A^i + l_B + l_{dil}^i \tag{24}$$

$$v^i = v_A^i + v_{CH4} + v_{dil}^i \tag{25}$$

The relationship between CO_2 molar flow rate in liquid and vapor phases leaving stage i is shown in Eq. (26). The loading in the liquid phase is calculated by employing the soft model[39] as a function of the CO_2 partial pressure in the vapor phase, which can be readily evaluated by Eq. (27). Here it is assumed that the pressure is constant throughout the absorber column, and this pressure p_{ABS} is equal to 1 bar (10^5 Pa).

$$l_A^i = l_B \cdot \alpha\left(p_A^i, T^i\right) \tag{26}$$

$$p_A^i = \frac{v_A^i}{v^i} \cdot p_{ABS} \tag{27}$$

Similarly, the partition of the diluent between gas and liquid phases can be evaluated by Raoult's law, Eq. (28).

$$p_{dil}^i = \frac{v_{dil}^i}{v^i} \cdot p_{ABS} = p^{sat}\left(T^i\right) \cdot \frac{l_{dil}^i}{l^i} \tag{28}$$

The absorber molar flow profiles can be solved iteratively. In stage i = 0, the top of the column, the liquid flow rate of CO_2 l_A^0 is defined by the lean loading of the absorbent whereas that of diluent l_{dil}^0 is calculated by considering that the solvent is a 30 %wt. solution of MEA plus diluent. At the bottom of the column, stage i = N+1, the vapor flow rate of CO_2 v_A^{N+1} is calculated by fixing a certain proportion CO_2/methane in the raw gas to be treated. The vapor flow rate of diluent v_{dil}^{N+1} is naturally null. All that remains to be solved is the energetic balance, Eq. (29).

$$l^{i-1} \cdot C_{P,L}^{i-1} \cdot T^{i-1} + v^{i+1} \cdot C_{P,V}^{i+1} \cdot T^{i+1} = l^i \cdot C_{P,L}^i \cdot T^i + v^i \cdot C_{P,V}^i \cdot T^i - E^i \tag{29}$$

In Eq. (29), the term E^i refers to the amount of energy released/absorbed at that particular stage of the column. The energy released refers to the heat of absorption of CO_2 in the solvent, here kept at ΔH = 85 kJ·mol CO_2^{-1} following the average of that obtained experimentally by Kim et al.[50,51], while the energy absorbed refers to the latent heat required to evaporate the diluent, which has been calculated by employing the Clausius-Clapeyron relationship particular for each diluent shown in Appendix 1. This is shown in Eq. (30).

$$E^i = \left(v_A^i - v_A^{i+1}\right) \cdot \Delta H + \left(l_{dil}^i - l_{dil}^{i-1}\right) \cdot L_{dil}^i \tag{30}$$

For this study, the equilibrium shift mentioned previously in Section 2.4 has been neglected as so not to complicate even further the discussion (in terms of Section 2, this means that all following analyses will rely on the CASE B scenario). The heat capacities of both vapor and liquid phases have been calculated with the parameters shown in Appendix 1 and the mixing rules described in Appendix 2. As mentioned previously, ΔH has been kept constant throughout all loadings of the solvent. This is not consistent with data obtained by Kim et al.[50,51], particularly because, at higher loadings, the mechanism for CO_2 absorption shifts from carbamate to bicarbonate formation – the former being more exothermic than the latter. However, to make our analysis consistent for water-lean solvents (where no bicarbonate formation is expected), we have decided to assume an invariant CO_2 heat of absorption.

3.2.Temperature bulge and CO_2 capture dependence on thermal phenomena

We might start by briefly discussing the expected results for these simulations. As mentioned, the partial pressure of the diluent in the vapor phase can be estimated by Raoult's law, with the saturation pressure (p^{sat}) of the diluent being the proportionality factor intermediating the relationship. For higher values of p^{sat} there will be more diluent evaporation and, consequentially, less temperature increase in the column. Conversely, higher heat capacities both in gas and liquid phases will also propitiate lower temperature increases. However, the discussion is a bit more complex than that, since the absorption of CO_2 itself is limited at higher temperatures, meaning that there is an unavoidable *cap* for how much heat release will be observed in an absorber column.

Figure 9 has been obtained by numerical simulation and illustrates the case of aqueous 30 %wt. MEA. The liquid-to-gas ratio L/G has been set as a function of the CO_2 concentration in the inlet gas, so that essentially the amine-to-CO_2 mass ratio is kept constant. In our simulations, L/G = 6.5 kg solvent·kg gas^{-1} for the case of an inlet gas with Y_{CO2} = 16.5 %v/v, which is a reasonable value following the example of Kvamsdal and Rochelle[49]. This ratio has been adjusted to represent L/G in terms of CO_2, so that L/G = 18.5 kg solvent·kg CO_2^{-1} for all cases. As Y_{CO2} increases, the temperature bulge increases in magnitude (T_{MAX} gets bigger) and slowly descends from the top of the column down to its bottom. For very high values of Y_{CO2}, T_{MAX} decreases again, and one ends up having a small temperature bulge at the bottom of the absorber. This behavior is consistent with that observed by Kvamsdal and Rochelle[49] despite the fact that our model is highly simplified.

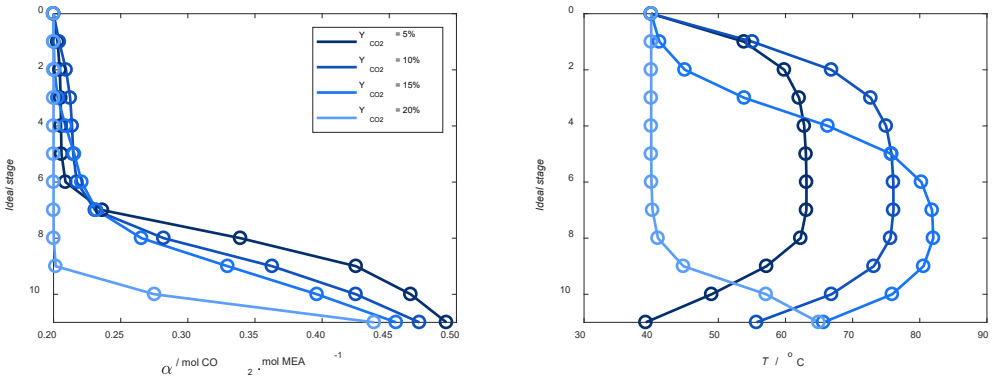

Figure 9. Profiles of CO_2 loading and temperature in each theoretical stage of the absorber when operating with aqueous 30 %wt. MEA (L/G = 18.5 kg solvent·kg CO_2^{-1}, lean loading α = 0.20 mol CO_2·mol MEA^{-1}, absorber with 10 equilibrium stages).

Figure 10 provides another visualization of the phenomenon that is being discussed here. As it can be seen, an increase in Y_{CO2} brings an increase (followed by a decrease) of T_{MAX} and a migration of the temperature bulge from the top to the bottom of the absorber. The percentage of CO_2 captured follows an increasing trend with increasing CO_2 partial pressures in the raw gas. The most harmful effect of the temperature bulge is to essentially slow down this increasing trend, something that can be readily observed in the *plateau* of the upper-right plot of Figure 10. It must be highlighted here that, by fixing parameters such as the L/G, the initial lean loading α and the number of equilibrium stages, we have arbitrarily defined the shape of this equilibrium plateau. Different parameters would clearly affect how quickly the temperature bulge shifts to the bottom of the column. However, for comparison purposes, it is enough to disregard these effects in the present moment.

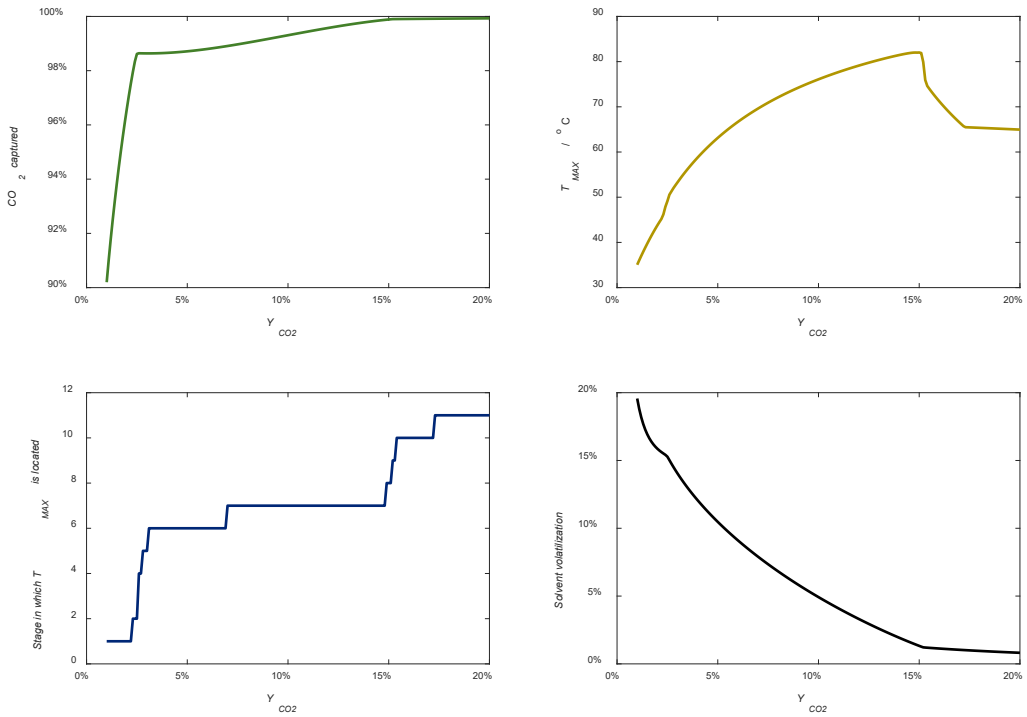

Figure 10. Curves for CO_2 captured, maximum temperature reached in absorber, equilibrium stage in which the maximum temperature is located, and solvent volatilization versus CO_2 content in raw gas stream when operating with aqueous 30 %wt. MEA (L/G = 18.5 kg solvent·kg CO_2^{-1}, lean loading α = 0.20 mol CO_2·mol MEA^{-1}, absorber with 10 equilibrium stages).

Another consideration to be taken when discussing thermal phenomena in the absorber is the amount of diluent lost at the top of the reboiler due to volatilization, which can also be seen on Figure 10 for the case of aqueous MEA. This diluent that escapes into the vapor phase is not gone, as real CO_2 capture plants employ a number of mechanisms to avoid losses, such as water wash sections and concentration columns[52] (as in the case of the Amisol process, where methanol volatilization is an issue). However, the increase in instrumentation and operational complexity brought by solvent volatilization makes this an issue worth considering when comparing different diluents for water-lean solvent formulation. This will be discussed a bit more in the following Section 3.3. As a final remark, we must reinforce that our model does not consider the volatilization of the amine itself, which means that by '*solvent loss*' or '*solvent volatilization*' we are talking only about the evaporation of the diluent itself, by far a lesser problem than amine volatilization for operational purposes.

3.3. Shifting thermal phenomena in water-lean solvents

Section 3.2 intended to show that the increase in temperature in the absorber is responsible for a relative loss in CO_2 capture capacity, and that such warming up is limited by the vaporization of the solvent itself. This sequence of events suggests that diluents with lower volatility than water will be subject to more heating than aqueous amines and, therefore, to an earlier and fiercer loss in CO_2 capture capacity. This is precisely what the results of this analysis show. The following results apply to columns designed with 5 equilibrium stages, a bit closer to practical applications than the 10 equilibrium stages employed in Section 3.2. Figure 9 demonstrates both the CO_2 captured in the absorber and the maximum temperature achieved in the column for a series of hypothetical water-lean solvents based on 30 %wt. MEA.

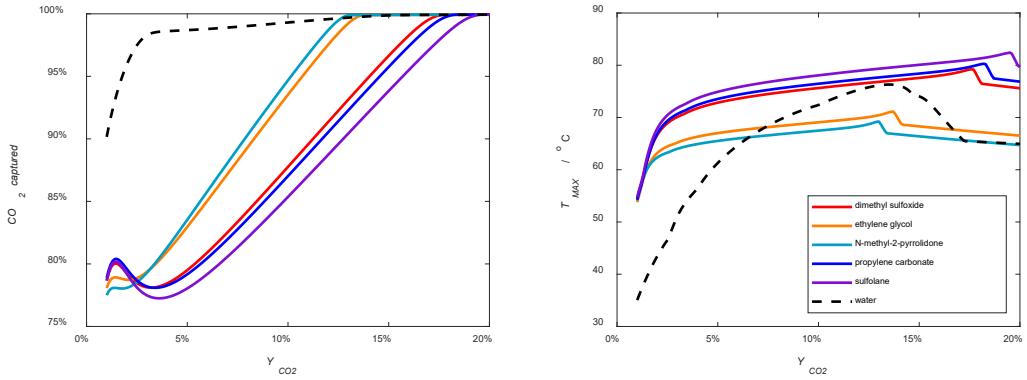

Figure 11. Curves for CO_2 captured and maximum temperature reached in absorber versus CO_2 content in raw gas stream when operating with water-lean solvents based on 30 %wt. MEA plus a series of miscellaneous organic diluents (L/G = 18.5 kg solvent·kg CO_2^{-1}, lean loading α = 0.20 mol CO_2·mol MEA^{-1}, absorber with 5 equilibrium stages).

The series of water-lean solvents shown in Figure 11 was specifically chosen due to their low volatility, following the suggestion given in Wanderley et al.[10] that this class of solvents might reduce reboiler heat duties in CO_2 capture plants. As it turns out, this same low volatility could be responsible for a clear limitation in CO_2 capture capacities depending on the CO_2 content of the raw gas. All water-lean solvents in this series are subject to more warming up in the absorber due to their low volatility, with sulfolane, propylene carbonate and dimethyl sulfoxide showing the worst performance. Solvents containing ethylene glycol and N-methyl-2-pyrrolidone are somewhat more volatile and, consequentially, less problematic, but still more vulnerable to loss of capacity due to thermal phenomena than aqueous MEA.

Diluents with higher volatility than water, on the other hand, introduce a different kind of problem. Figure 10 exemplifies the effects of thermal phenomena in a series of ketone-based

water-lean solvents very similar to the one shown previously in Section 2.7, Figure 4. For ketones less volatile than water, such as cyclopentanone and cyclohexanone, the same behavior observed in Figure 11 can be seen again (increased T_{MAX} denoting more warming up in the absorber column and an earlier loss of CO_2 capacity dependent on the CO_2 content in the raw gas). Conversely, water-lean solvents containing acetone and methyl ethyl ketone suffer less warming up than aqueous 30 %wt. MEA due to their high volatility. The result is that they are theoretically able to sustain the absorption of more CO_2 even at increased amounts of impurities in the raw gas. However, this comes at the price of solvent evaporation. For low Y_{CO2}, the evaporation of acetone and methyl ethyl ketone approaches 100 % in water-lean solvents. At these rates of evaporation, it is impossible to suggest that the vapor-liquid equilibrium behavior of these solvents still follows anything close to the soft model parametrized for aqueous MEA.

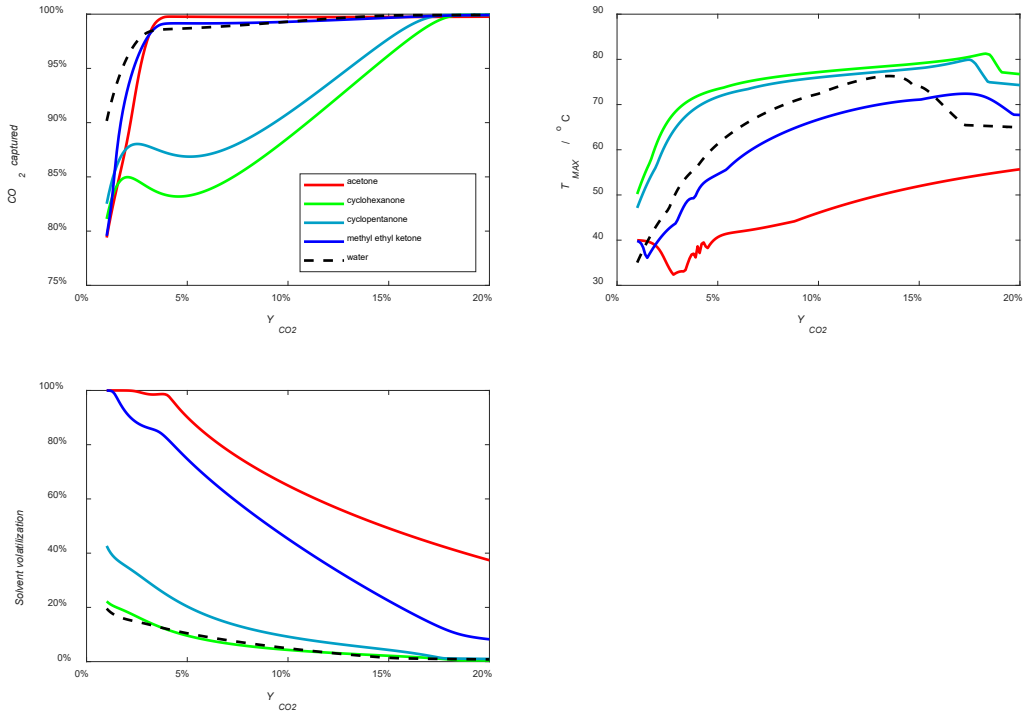

Figure 12. Curves for CO_2 captured, maximum temperature reached in absorber and solvent volatilization versus CO_2 content in raw gas stream when operating with water-lean solvents based on 30 %wt. MEA plus a series of ketones (L/G = 18.5 kg solvent·kg CO_2^{-1}, lean loading α = 0.20 mol CO_2·mol MEA^{-1}, absorber with 5 equilibrium stages).

Figure 11 and Figure 12 highlight the two sides of choosing diluents with volatilities different than that of water. On one hand, if the volatility is too low, there is a chance that thermal phenomena in the absorber will limit the capacity for capturing CO_2, and particularly so if the

amount of CO_2 in the raw gas stream is high. This means that this brand of low-volatility water-lean solvents should probably be deployed with sophisticated intercooling mechanisms, so that the absorber can be made to perform as close to isothermal as possible. On the other hand, high-volatility water-lean solvents will require efficient solvent-washing, recuperation and concentration strategies to prevent the enormous losses observed in Figure 10. In both cases, merely adopting the technology employed for aqueous solvents in a water-lean solvent context would not be enough.

Table 4 gives a glimpse of the thermal phenomena in hypothetical water-lean solvents with the various solvents based on 30 %wt. MEA considered in Table 3 of Section 2.7. It underlines the issues related to high temperatures obtained in many of the diluents with low volatility and the theoretical losses associated with very volatile diluents.

Table 4. Comparison between maximum temperature and solvent loss in the absorber when employing hypothetical solvents based on 30 %wt. MEA (L/G = 18.5 kg solvent·kg CO_2^{-1}, lean loading α = 0.20 mol CO_2·mol MEA^{-1}, absorber with 5 equilibrium stages).

Name	Y_{CO2} = 5 %v/v		Y_{CO2} = 10 %v/v	
	T_{MAX} / °C	Solvent loss*	T_{MAX} / °C	Solvent loss*
acetone	41	90 %	46	65 %
benzaldehyde	74	4 %	77	2 %
n-butanol	66	15 %	69	6 %
2-butanol	64	35 %	75	19 %
t-butanol	42	27 %	41	12 %
cyclohexanol	70	3 %	72	1 %
cyclohexanone	73	10 %	77	4 %
cyclopentanone	72	20 %	76	9 %
dimethyl sulfoxide	73	0 %	76	0 %
dimethyl formamide	72	8 %	76	4 %
ethanol	49	39 %	60	19 %
ethylene chloride	—	100 %	—	100 %
ethylene glycol	67	0 %	69	0 %
glycerol	68	0 %	70	0 %
heptanol	60	1 %	62	0 %
hexanol	61	3 %	63	1 %

isoamyl alcohol	62	6 %	64	2 %
isobutanol	60	18 %	63	5 %
isopropanol	58	55 %	65	21 %
methanol	35	33 %	43	23 %
methyl ethyl ketone	55	75 %	67	45 %
nitrobenzene	75	1 %	78	1 %
N-methyl-2-pyrrolidone	66	0 %	67	0 %
pentanol	61	5 %	63	2 %
propanol	61	32 %	68	12 %
propionitrile	62	37 %	74	21 %
propylene carbonate	74	1 %	76	0 %
pyridine	69	35 %	77	18 %
sulfolane	75	0 %	78	0 %
water	61	10 %	72	5 %

* Solvent loss here means merely the amount of vaporized diluent that leaves in the top of the column, which can be readily separated by washing and/or cooling and returned to absorber.

Once we have decided to fix a relationship between L/G and Y_{CO2}, the results in this Section 3.3 follow as a consequence. Meanwhile, Kvamsdal and Rochelle[49] have remarked the existence of a critical L/G around which the effects of the temperature bulge have a sensible impact on the absorption performance of a solvent. It is plausible that a big part of the loss of CO_2 capture capacity seen on Figure 11 for low-volatility solvents could be addressed by simply employing larger liquid-to-gas ratios for these solvents at low Y_{CO2} conditions. Similarly, higher liquid-to-gas ratios would minimize the solvent vaporization issues observed for high-volatility solvents (a fact mentioned by Kohl and Nielsen regarding the Amisol process technology[53]). A high L/G is likely to increase the overall costs of CO_2 capture if no trade-offs can be found elsewhere.

In this Section 3, we have mentioned that the heat capacities of the diluent both in the vapor and in the liquid phases might influence the thermal phenomena in the absorber without delving into further details. This particular issue has been addressed in the Supporting Information material. Indeed, the heat capacities C_P have relatively small impacts on thermal phenomena when compared with p^{sat}. However, since both C_P of the liquid and p^{sat} play an important role

in the discussion carried in Section 4, it might be too early to take conclusions regarding the relative importance of either parameter.

4. Reboiler heat duties

The reboiler of the stripper is responsible for supplying the energy required for CO_2 desorption. We have extended our analysis to evaluate which solvent parameters will effectively impact the performance of the reboiler, and therefore which diluent parameters one should be attentive to when screening possibilities for water-lean solvents.

This analysis relies on the assumption that the CO_2 heat of absorption in water-lean solvents is either the same or very similar to that in aqueous amine solvents. This has been one of the main results obtained through experimentation in Wanderley et al.[10], and is consistent with the theory of carbamate formation being the main exothermic process during CO_2 absorption in amine systems. However, as it has been suggested in that study, water-lean solvents might still bring a reduction in reboiler heat duties due to their low volatility and lower heat capacities. The goal of Section 4 is analyzing if that is indeed the case or if, as suggested by Yuan and Rochelle[15], the diminishing heat transfer performance of water-lean solvents due to high viscosities and low heat conductivities far outweighs those benefits.

Similarly to what has been done in Section 3, the present study applies only for nonaqueous water-lean solvents, as we have little means to evaluate how the activity coefficient of water (and thus its volatility) would behave in semi-aqueous water-lean solvents. It is plausible that water volatility would be higher in organo-amine mixtures, which would bring higher latent heat expenditures while at the same time addressing the issue highlighted in Section 4.3. Section 4.3 puts into a new perspective much of the calculations performed in Sections 4.1 and 4.2. We believe that, rather than undermining our own conclusions, this new perspective builds upon our discussion and complements it, in a '*Wittgenstein's ladder*' type of approach.

4.1. Heat recovery in the cross-heat exchanger

Before entering the reboiler, some heat can be recovered from the hot lean amine stream coming from the desorber in a cross-heat exchanger. Therefore, the temperature of the rich amine stream that enters the reboiler is not that of the amine leaving the absorber (T_0 = 60 °C has been fixed so as to reach a compromise between the different cases presented in Section 3) but a higher value T_X. T_X is defined by the temperature of the hot lean amine stream T_H and by

the area in the cross-heat exchanger. In this work, an ideal T_X is assumed to be T_X = 105 °C following Xu et al.[54].

In a previous study, Lin and Rochelle[55] have performed a parametric optimization of the cross-heat exchanger in the context of CO_2 capture from which this analysis will draw heavily. As those authors pointed out, optimum operation of this unit is dependent on solvent properties such as heat capacity and viscosity. However, their findings were applied to the context of reducing capital and operational costs. Conversely, our analysis will be divided into two different scenarios, CASE C and CASE D.

- CASE C – This scenario assumes that the CO_2 capture plant already exists, meaning that its capital costs are fixed. The existing capture plant has been designed for traditional solvents, so that the area available for heat transfer will be evaluated for T_X = 105 °C when using aqueous absorbents. Once this area is calculated, it will be kept constant while studying different organic diluents. As it will be seen in this approach, T_X is typically lower than 105 °C, which translates into more sensible heat expenses in the reboiler.
- CASE D – In this scenario, we consider that a new heat exchanger of different area could be installed to deal with the heating of the rich amine up to T_X = 105 °C. This unit will be bigger than that used for warming up the aqueous solvent, though calculation of how this impacts the capital costs of the CO_2 capture plant is beyond the scope of this study. Overall, the results of this analysis will be more optimistic than those of CASE C.

The amount of heat that can be transferred in the cross-heat exchanger is given by Eq. (31).

$$Q_{HX} = U_{HX} \cdot A_{HX} \cdot \Delta T_{lm} \tag{31a}$$

$$Q_{HX} = C_P \cdot q \cdot (T_X - T_0) \tag{31b}$$

In Eq. (31a), U_{HX} is the overall heat transfer coefficient, A_{HX} is the area available for heat exchange and ΔT_{lm} is the log mean temperature difference between rich and lean streams. Eq. (31b) is also true, since the heat transferred in the unit is responsible for raising the temperature of the rich stream from T_0 up to T_X. This stream has a mass flow rate of q and a heat capacity of C_P. Equality between Eqs. (31a) and (31b) results in Eq. (32) for the exit temperature of the rich stream.

$$T_X = T_0 + \frac{U_{HX} \cdot A_{HX} \cdot \Delta T_{lm}}{C_P \cdot q} \tag{32}$$

Following the approach of Lin and Rochelle[55], one can consider this equipment to be a plate-and-frame type exchanger (PHE), and the following derivations will be based both on that work as on Dhar[56]. Assuming a PHE with plate-spacing D_{HX}, plate-width W_{HX}, plate height H_{HX} and number of plates N_{HX}, the mass flow rate of rich solvent q can be calculated by Eq. (33). Meanwhile, Eq. (34) expresses the area available for heat transfer. With Eqs. (32)–(34), one can obtain Eq. (35).

$$q = \rho \cdot u \cdot D_{HX} \cdot W_{HX} \cdot N_{HX} \tag{33}$$

$$A_{HX} = H_{HX} \cdot W_{HX} \cdot N_{HX} \tag{34}$$

$$T_X = T_0 + \frac{U_{HX} \cdot H_{HX} \cdot \Delta T_{lm}}{\rho \cdot C_P \cdot D_{HX} \cdot u} \tag{35}$$

Lin and Rochelle[55] have assumed that the resistance to heat transfer in the PHE plates is negligible. Furthermore, they propose that the convective heat transfer coefficients h of both rich and lean streams can be averaged. Following this approach, Eq. (36) suggests that the global heat transfer coefficient of the PHE is half the convective heat transfer coefficient evaluated at the average temperature between rich and lean amine streams.

$$\frac{1}{U_{HX}} \approx \frac{2}{h} \tag{36}$$

Substitution of Eq. (36) into Eq. (35) yields Eq. (37).

$$T_X = T_0 + \frac{1}{2} \cdot \frac{h \cdot H_{HX} \cdot \Delta T_{lm}}{\rho \cdot C_P \cdot D_{HX} \cdot u} \tag{37}$$

The convective heat transfer coefficient h can be obtained by using the three nondimensional numbers Nusselt (Nu), Reynolds (Re) and Prandtl (Pr) (Eqs. 38–40) and a suitable correlation, expressed generically in Eq. (41), where C_{Nu}, m and n are empirical parameters. Notice that, in these equations, the characteristic length of the PHE is $2 \cdot D_{HX}$, or two times the spacing between plates.

$$Re = \frac{2 \cdot \rho \cdot D_{HX} \cdot u}{\eta} \tag{38}$$

$$Pr = \frac{C_P \cdot \eta}{\lambda} \tag{39}$$

$$Nu = \frac{2 \cdot h \cdot D_{HX}}{\lambda} \quad (40)$$

$$Nu = C_{Nu} \cdot Re^{m} \cdot Pr^{n} \quad (41)$$

With Eqs. (38)–(41), the convective heat transfer coefficient h can be approximated by Eq. (42). Finally, Eq. (43) shows how the exit rich solvent temperature T_X can be calculated. Notice in Eq. (43) that the first few terms of that expression are related either to the dimensions of the equipment (D_{HX}, L_{HX}) or to how one chooses to operate the process (u, ΔT_{lm}), whereas the solvent properties ρ, C_P, λ and η appear in the end. As for the empirical parameters C_{Nu}, m and n, a good overview of their values has been catalogued by Lin and Rochelle[55]. A common thread among the alternatives is that m and n are always numbers between 0 and 1 and m > n, meaning that T_X increases with λ and decreases with ρ, C_P and η for a fixed process configuration and operational conditions.

$$h = C_{Nu} \cdot (2 \cdot D_{HX})^{m-1} \cdot u^{m} \cdot \rho^{m} \cdot {C_P}^{n} \cdot \lambda^{1-n} \cdot \eta^{n-m} \quad (42)$$

$$T_X = T_0 + C_{Nu} \cdot (2 \cdot D_{HX})^{m-2} \cdot H_{HX} \cdot u^{m-1} \cdot \Delta T_{lm} \cdot \rho^{m-1} \cdot {C_P}^{n-1} \cdot \lambda^{1-n} \cdot \eta^{n-m} \quad (43)$$

The choice between the models presented by Lin and Rochelle[55] should not be a big concern in this analysis. It has been shown by those authors that, although the estimated Nu can vary greatly depending on the chosen correlation, its dependency on Re and Pr does not change too much among different models. Therefore, for comparisons between aqueous and water-lean solvents, the Nusselt correlation one picks is not that relevant. In the remainder of the calculations in this section, it is assumed that the model of Okada et al.[57] for PHE with corrugation angle of 30 ° can be employed, meaning C_{Nu} = 0.157, m = 0.66 and n = 0.4. Also following Lin and Rochelle[55], one can consider D_{HX} = 0.002 m and ΔT_{lm} = 5 °C.

According to Lin and Rochelle[55], the fluid velocity inside the cross-heat exchanger is typically between u = 0.32 and 0.42 $m \cdot s^{-1}$. For a fixed amount of energy transferred, higher values of u will demand a larger A_{HX} whereas lower velocities require smaller equipment. For the sake of comparison, it is assumed that u = 0.4 $m \cdot s^{-1}$.

Table 4 shows the results of CASE C and CASE D with different water-lean solvents based on 30 %wt. MEA when compared with the aqueous amine solvent. The parameters ρ, C_P, λ and η were obtained as functions of temperature for all organic diluents plus MEA, as shown in Appendix 1, and then treated with the mixing rules presented in Appendix 2. The effects of CO_2 loading in these properties have been neglected for the present analysis.

Table 5. Comparison between the performance of the PHE using different hypothetical solvents based on 30 %wt. MEA.

Name	CASE C: T_X calculated / °C	CASE D: A_{HX} increment for T_X = 105 °C
acetone	89	+56 %
benzaldehyde	81	+112 %
butanol	80	+118 %
2-butanol	80	+116 %
t-Butanol	78	+134 %
cyclohexanol	73	+209 %
cyclohexanone	79	+124 %
cyclopentanone	91	+43 %
dimethyl sulfoxide	79	+126 %
dimethyl formamide	85	+77 %
ethanol	83	+89 %
ethylene chloride	87	+71 %
ethylene glycol	78	+127 %
glycerol	71	+256 %
heptanol	76	+173 %
hexanol	77	+156 %
isoamyl alcohol	78	+136 %
isobutanol	77	+153 %
isopropanol	79	+132 %
methanol	90	+49 %
methyl ethyl ketone	85	+75 %
nitrobenzene	79	+128 %
N-methyl-2-pyrrolidone	77	+152 %
pentanol	78	+144 %
propanol	80	+113 %
propionitrile	88	+58 %
propylene carbonate	79	+124 %
pyridine	85	+78 %
sulfolane	76	+171 %

water	105	+0 %

As evidenced in Table 5 and already predicted by Yuan and Rochelle[15], shifting from aqueous to water-lean solvents has an enormous impact on the performance of the PHE. This has three main reasons. The first one is the high viscosity of a good number of organic diluents. The second is that all of these diluents have heat capacities lower than that of water when taken in mass basis. The third, vastly overlooked, is the thermal conductivity of the diluent. These three factors strongly affect the performance of the PHE, and we have carried an analysis on the impact of each different parameter in Appendix 5. The takeaway is that, for water-lean solvents based on N-methyl-2-pyrrolidone or sulfolane for example, this implies either accepting that the rich amine can only be heated up to about 77 °C instead of 105 °C (CASE C), or that the cross-heat exchanger must be more than twice its original size (CASE D).

4.2. Evaluating reboiler heat duties using a shortcut approach

After passing through the cross-heat exchanger, the rich amine stream is fed to the reboiler, where it is heated with compressed steam. This heating is responsible for three distinct tasks:

1. Increasing the temperature from that of the reboiler feed (T_X) up to that of desorption (T_R), typically around T_R = 120 °C for aqueous MEA – often called sensible heat;
2. Vaporizing the diluent, which is not only inevitable (as some of the diluent will surely volatilize at high temperatures) but also important for helping stripping CO_2 – often called latent heat;
3. Reversing the reaction between CO_2 and amine, thus desorbing CO_2 from the solvent – often called absorption heat.

Oexmann and Kather[16] have arrived at the following Eq. (44) for the calculation of the reboiler heat duty of a CO_2 capture plant.

$$Q_R = \frac{C_P \cdot (T_R - T_X)}{\Delta\alpha} \cdot \frac{M}{M_A} \cdot \frac{1}{x_B} + L_{dil} \cdot \frac{p_{dil}}{p_A} \cdot \frac{1}{M_A} + \frac{\Delta H}{M_A} \tag{44}$$

Eq. (44) can be further simplified if one defines Δq as the mass cyclic capacity of CO_2 in the solvent following Eq. (45). This results in Eq. (46).

$$\Delta q = \frac{M_A}{M} \cdot x_B \cdot \Delta\alpha \tag{45}$$

$$Q_R = \frac{C_P \cdot (T_R - T_X)}{\Delta q} + \frac{\sum L_i \cdot p_i}{p_A \cdot M_A} + \frac{\Delta H}{M_A} \quad (46)$$

Eq. (46) shows how the reboiler duty per mass of CO_2 captured can be obtained as a function of the solvent heat capacity C_P, the latent heat and partial pressure L_i and p_i of all diluents at stripper temperature, the CO_2 partial pressure and molar mass p_A and M_A, the heat of absorption ΔH and the difference between the temperatures T_R at the reboiler and T_X at the cross-heat exchanger. The partial pressure of the diluents can be calculated by using Raoult's law with the saturation pressure p^{sat} of the pure diluents at 120 °C, which have been calculated with the parameters presented in Appendix 1 and shown on Table 5.

Wanderley et al.[10] have shown that the cyclic capacity in water-lean solvents can, in theory, be the same or even higher than that of aqueous solvents. Also following that work, and just as we did in Section 3, the heat of absorption of CO_2 is fixed for both aqueous and water-lean solvents at ΔH = 85 kJ·mol CO_2^{-1}. We have also assumed that CO_2 can be recovered in the reboiler at 1 bar ($p_A = 10^5$ Pa), which can theoretically be achieved either by heating or by flushing with an inert gas. A discussion on these two hypotheses will be carried in the next Section. For now, if one assumes that $\Delta\alpha$ = 0.3 mol CO_2·mol MEA^{-1} (or conversely 65 g CO_2·kg solution^{-1} in a 30 %wt. MEA solvent), Table 6 shows how the reboiler heat duties will decrease or often increase when shifting from aqueous to water-lean solvents.

Table 6. Comparison between reboiler duties using different hypothetical solvents based on 30 %wt. MEA (T_X varies in CASE C, T_X = 105 °C in CASE D, T_R = 120 °C, $p_A = 10^2$ kPa).

Name	p^{sat} at 120 °C / kPa	CASE C: Q_R increment	CASE D: Q_R increment
acetone	620.2	+39 %	+24 %
benzaldehyde	17.6	−25 %	−43 %
butanol	110.7	+1 %	−24 %
2-butanol	211.6	+10 %	−13 %
t-butanol	363.5	+33 %	+5 %
cyclohexanol	25.7	−12 %	−39 %
cyclohexanone	35.4	−20 %	−40 %
cyclopentanone	73.5	−23 %	−35 %
dimethyl sulfoxide	2.0	−24 %	−44 %

dimethyl formamide	37.5	−22 %	−39 %
ethanol	413.1	+45 %	+22 %
ethylene chloride	1454.5	+69 %	+57 %
ethylene glycol	4.3	−15 %	−41%
glycerol	0.0	−10 %	−42 %
heptanol	14.9	−4 %	−37 %
hexanol	29.4	−7 %	−36 %
isoamyl alcohol	68.7	−1 %	−30 %
isobutanol	155.5	+14 %	−17 %
isopropanol	360.9	+41 %	+11 %
methanol	642.3	+71 %	+56 %
methyl ethyl ketone	319.4	+10 %	−8 %
nitrobenzene	5.9	−27 %	−45 %
N-methyl-2-pyrrolidone	5.9	+2 %	−35 %
pentanol	54.8	−2 %	−32 %
propanol	219.6	+18 %	−8 %
propionitrile	199.9	−2 %	−17 %
propylene carbonate	3.7	−26 %	−45 %
pyridine	115.8	−16 %	−31 %
sulfolane	0.5	−23 %	−45 %
water	199.0	+0 %	+0 %

Table 5 shows that water-lean solvents with low volatility (i.e. based on organic diluents less volatile than water) might often offer benefits in terms of reboiler duties when a specific heat-exchanger with large area A_{HX} is designed to recover energy from the hot lean amine (CASE D). Such is the case with ethylene glycol, N-methyl-2-pyrrolidone, propylene carbonate and sulfolane. This is even the case for excessively viscous solvents such as glycerol. However, when the issues regarding heat transfer in the PHE are taken into account (CASE C), many of these solvents underperform because of the extra amount of sensible heat required to compensate the shortcomings of the cross-heat exchanger.

Overall, however, the results presented on Table 5 are quite positive for water-lean solvents. Even diluents which have clear issues in terms of heat transfer in the PHE, such as sulfolane (T_X = 76 °C), might be able to provide savings in reboiler heat duties following CASE C just

by force of their low volatility. This is because sensible heat in the reboiler is a small fraction of the total heat expenditures, with latent heat playing a more significative part. Therefore, the diluent p^{sat} has a stronger impact in reboiler duty analyses than any other variable. A more in-depth discussion of the impact of each variable can be seen in Appendix 5.

4.3. The issue with reboiler pressures in solvents with low volatility

The liquid stream coming out of the reboiler is the lean solvent, which is later recirculated back to the absorber. In the reboiler, this lean solvent is in equilibrium with a vapor containing solvent and CO_2 at a certain pressure p_R. This pressure will then limit the operability of the reboiler. In other words, the vapor-liquid equilibrium behavior of the solvent will always tie together the composition of the lean solvent and the pressure of the reboiler.

Wanderley et al.[10] have obtained VLE curves for a variety of water-lean solvents at 120 °C. For the moment we shall focus our attention on solvents with low volatility such as N-methyl-2-pyrrolidone, as it has been demonstrated in Section 4.2 that these are the ones most likely to provide lower reboiler duties. The VLE behavior of NMP + 30 %wt. MEA has been compared to that of aqueous 30 %wt. MEA at 120 °C in Figure 13.

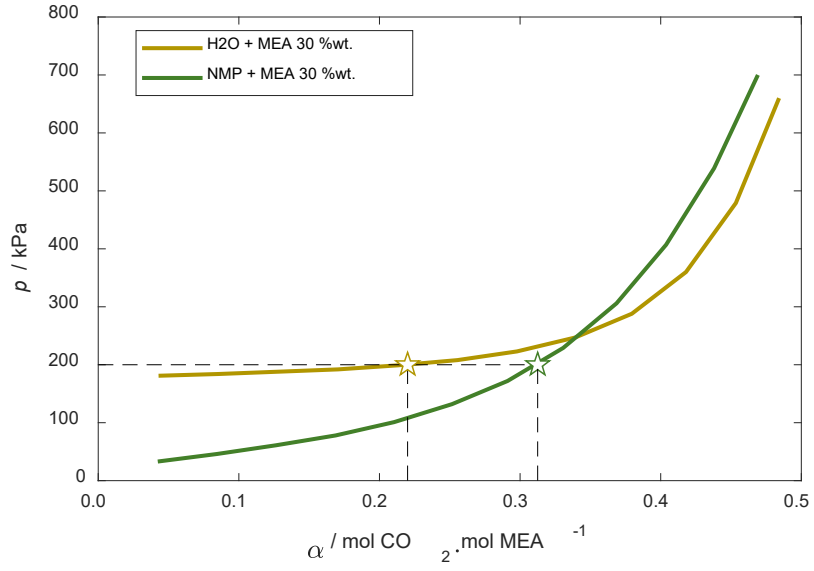

Figure 13. Vapor-liquid equilibrium curves of aqueous 30 %wt. MEA and NMP + 30 %wt. MEA both at 120 °C. The stars identify the lean loadings in equilibrium with p_R = 200 kPa. Image adapted from data published in Wanderley et al.[10].

Supposing one wants to produce a lean solvent with α = 0.2 mol CO_2·mol MEA^{-1}, the operational pressure of the reboiler with aqueous 30 %wt. MEA at 120 °C is of p_R = 195 kPa.

This is a feasible scenario. For NMP + 30 %wt. MEA, however, the operational pressure is p_R = 95 kPa, a sub-atmospheric condition.

This imposes a series of limitations for water-lean solvents with low volatility. If one wants to actually recover the solvent with the same lean loading as that of aqueous MEA, they will need to resort to different strategies. One possible strategy would be elevating the temperature of the reboiler above 120 °C. However, what prevents the operation of the reboiler at higher temperatures is the degradation of the solvent, and it has been previously assessed by our group[58] that primary amines in water-lean solvents are more vulnerable to thermal degradation (and possibly oxidative degradation) than when in aqueous solutions. Another alternative is employing an inert stripping gas, something already suggested by Rivas and Prausnitz in 1979[7], or at least a non-reactive co-solvent with high volatility such as suggested by Frimpong et al.[59]. And then again, adding a volatile liquid to the mixture seems to defeat the purpose of choosing a water-lean solvent with low volatility to begin with. A stripping gas might then be a feasible solution, with the caveat that the CO_2 henceforth produced at the top of the desorber will most likely not be pure enough for storage.

For recovering high-purity CO_2 ready for storage or utilization when employing a low-volatility nonaqueous solvent, we can finally propose two alternatives with very clear handicaps. The first is to recover the solvent by operating the desorber under sub-atmospheric conditions, i.e. by vacuum stripping, with an obvious penalty in electrical power. This seems to be the approach adopted by some researchers working with ionic liquids[60] (many proposals for CO_2 regeneration after capture by ionic liquids can be operated at 100 kPa, but only because absorption itself is carried at very high pressures, so that the full potential of a pressure-swing can be attained[61–63]). The second is to recover a lean solvent with higher loading than that of aqueous amines.

If one fixes the pressure of the reboiler at p_R = 200 kPa and T_R = 120 °C, that will imply a lean loading of α = 0.31 mol CO_2·mol MEA^{-1} for NMP + 30 %wt. MEA (against α = 0.22 mol CO_2·mol MEA^{-1} for aqueous 30 %wt. MEA), as seen on Figure 11. This is a significative increase. As mentioned in Section 2.7, due to the vapor-liquid equilibrium shift in water-lean formulations, these solvents are already operating with lower rich loadings in the absorber. If the lean loading must be higher as well, this means that the cyclic capacity of water-lean solvents is lower than that of aqueous amines. The consequence is that more liquid is required to capture the same amount of CO_2, which not only jeopardizes any benefit acquired in terms

of mass transfer coefficients as discussed in Section 2, but will also increase the reboiler duties calculated in 4.2 under assumption of comparable cyclic capacities Δq.

The present analysis has been carried for the case of NMP + 30 %wt. MEA. A similar analysis could be made with other solvents of very low volatility, such as MEG or THFA, both presented by Wanderley et al.[10]. For solvents with lower volatility than water but higher than NMP, such as the 2-methoxyethanol (a.k.a. methyl cellosolve) studied by Guo et al.[41], one could possibly find a compromise between lower vaporization heat and the capacity of regenerating the solvent at higher pressures. Conversely, the addition of some water to a water-lean solvent may moderately increase its mass transfer coefficient and provide just enough steam in the reboiler so that the lean amine can be recovered at atmospheric pressures without excessive solvent volatilization. This seems to be the approach adopted by Semenova and Leites[13] for their water-lean solvents evaluated in pilot plant conditions, and also by the semi-aqueous solvents developed by ION Engineering[64] among others.

We have offered in this Section 4.3 several possible solutions to deal with CO_2 recovery in loaded water-lean solvents, each of them with its caveats. It is our opinion that this deadlock can perhaps be avoided by simple addition of some water to these solvents, generating semi-aqueous organo-amine mixtures. And yet again, some nonaqueous solvents can be formulated so that their volatility is just high enough for conventional regeneration, such as that of Guo et al.[41].[65] This discussion intends only to highlight the challenges posed to the utilization of water-lean solvents so that they can be more easily overcome.

5. Beyond the parametric analysis: chemistry in water-lean solvents

In the course of this study, we have treated all organic diluents alike. No comments were made regarding their chemical functionality, whether they are alcohols or ketones, aldehydes or halogenates. This was done with the intent of not further complicating our discussion, while also enabling us to look at a set of diluents large enough so that its analyses could be insightful.

However, all chemicals are not alike. In fact, as investigated previously by our group[10], it turns out that esters and ketones react pretty quickly with MEA, leading either to phase separation followed by a series of degradation reactions upon CO_2 absorption or simply to degradation when mixing with the amine directly. A more in-depth discussion on the proposed mechanisms in action can be found in that publication. The fact is that the elimination of esters and ketones preemptively retires many of the candidates from the pool of possibilities for water-lean solvent formulation.

For different reasons, aldehydes and halogenates should be retired as well. Aldehydes because of their inevitable reaction with amines, which can lead to a myriad of products[66]. Meanwhile, the chlorine content in pilot plant solvents has been shown to follow a suspicious synchronicity with their degradation levels[67,68]. This may be a good indicator that halogenates should be avoided. Another risk mentioned in literature is that of amine alkylation, a substitution reaction that can happen between halogenates and amines[69].

Now that these chemical functions have been eliminated, one is left with a more manageable row of options. It might now be warranted to treat some of the most obvious ones directly. Propylene carbonate has been observed in our experimental studies to react with MEA, being unsuitable for water-lean solvent formulation with primary amines. Coincidentally, Karlsson et al.[70] have recently reported suspicions of a reaction happening between propylene carbonate and 2-amino-2-methyl-1-propanol (AMP), as well. A reaction mechanism between propylene carbonate and MEA has also been proposed by Rivas and Prausnitz[7]. On the other hand, sulfolane is well known to induce phase separation in amino-mixtures upon CO_2 absorption[10,45,54,71,72].

Phase separation has also been observed in our experiments with N-formyl-morpholine unless the water-to-diluent proportion was elevated enough. It is worth pointing out that Leites[3] has directly correlated the phase-splitting observed in water-lean solvents with the dielectric permittivity of its organic diluent, pointing out that diluents with $\varepsilon > 23$ should fare well in avoiding biphasic solutions. The dielectric permittivity of N-formyl-morpholine at 25 °C is 24.3 (see Appendix 1), right at the limit. Our results show that Leites[3] is probably wrong by a few unities, but also that it is possible to account for this issue if the organic diluent is soluble enough in water.

In the meantime, experimentation is fundamental. The parametric analyses outlined in this study serve the purpose of pointing out what are the important aspects in terms of physical properties when looking at alternatives for water-lean solvent formulation, but chemical intelligence is still key in eliminating outlandish candidates, and practical laboratory work is what will eventually define whether a diluent is really promising or not.

6. Conclusions

It has been said before[4] that one of the biggest advantages in shifting from aqueous to water-lean solvents is the freedom in being able to choose the right diluent to tune in the properties

of the absorbent. This freedom can seem overwhelming. However, as shown in this work, the room for maneuver is quite more limited than it appears to be initially.

Section 2 shows that there is a clear trade-off between viscosity and CO_2 solubility when one focuses on mass transfer enhancement, meaning that one should probably not spend too much effort looking into a diluent if its viscosity exceeds a certain limit – about 7 to 8 mPa·s to be more precise, at least in the case of 30 %wt. MEA. Electrostatic phenomena are still important when looking into water-lean solvents, and in this work the dielectric permittivity has merely taken the role of a placeholder in lieu of more sophisticated relationships. However, even when this uncertainty source is accounted for, solvent viscosity still seems to be the main agent dragging down mass transfer rates.

Thermal phenomena in the absorber is an issue that is not frequently mentioned in works treating on water-lean solvents, the studies by Heldebrant et al.[1,6] being a clear exception. This should change, as it has become clear in Section 3 that any new diluent will bring more requirements to the absorber. If its volatility is too low, intercooling will be required to avoid overheating and sustain high CO_2 capture performance. If it is too high, solvent recovery becomes an issue. At any rate, both scenarios can be overcome with structural modifications in the absorber, but nevertheless require careful consideration.

The reboiler heat duties in carbamate-forming solvents seems to be a more challenging problem. As Yuan and Rochelle[15] have shown before, the lower heat conductivities and higher viscosities typical of all water-lean solvents prove to be an issue when designing the cross-heat exchanger. And even if its design is indeed revamped, with the associated capital expenditures, there is still the issue of how to extract the CO_2 out of a solvent if its volatility is too low. Section 4 has dealt with this dilemma, particularly in Section 4.3, which perhaps sheds a new light on the over-optimistic assumptions of our previous work[10].

Section 5 addresses the final issue of chemical knowledge being indispensable for delving into water-lean solvent formulation, warning finally that all previous parametric analyses cannot do without it.

Indeed, it seems that, with the equilibrium shift observed in water-lean solvents acting in the absorber, plus the troubles with thermal phenomena also in the absorber, plus the desorption issues investigated in the reboiler, it is hard to ascertain that water-lean solvents could deliver cyclic capacities comparable to aqueous amines without an overhaul of the CO_2 capture loop. At the same time, there are many possible formulations for water-lean solvents, and so the

discovery of a '*Goldilocks range*'[6] could possibly mean that a strong candidate can be discovered in the future. At any rate, we expect that this present study can be useful for researchers looking into developing water-lean solvents and, hopefully, overcoming the difficulties discussed here.

Supporting Information

The simulation work on water-lean solvents presented in this work relies on many parameters concerning previously published data available in literature, as well as a myriad of empirical correlations also available in literature. Sections 1 and 2 of the Supporting Information appendix sources and summarizes this data. Sections 3, 4 and 5 extend and give an in-depth assessment of the parametric analyses regarding mass transfer rates, thermal phenomena and heat of regeneration in water-lean solvents, complementing the discussion presented in the main manuscript. This information is available free of charge via the Internet at http://pubs.acs.org/.

Table of symbols

Symbols	Meaning	Units in the S.I.
A_{HX}	Area of the cross-heat exchanger	m^3
C	Concentration	$mol \cdot m^{-3}$
C_{Nu}	Parameter for Nusselt number correlation	
C_P	Heat capacity	$J \cdot mol^{-1} \cdot K^{-1}$
D	Diffusivity	$m^2 \cdot s^{-1}$
D_{HX}, H_{HX}, W_{HX}	Dimensions of the cross-heat exchanger	m
E	Energy	J
h	Convective heat transfer coefficient	$W \cdot m^{-2} \cdot s^{-1}$
h_+, h_-, h_g	Van Krevelen coefficients	
H	Henry's coefficient	$Pa \cdot m^3 \cdot mol^-$
I	Ionic strength	$mol \cdot m^{-3}$
k_2	Forward reaction kinetic rate constant	$m^3 \cdot mol^{-1} \cdot s^{-1}$
k_b/k_{-1}	Relative rate for zwitterion decomposition	$m^3 \cdot mol^{-1}$
k_g^*	Liquid phase mass transfer coefficient	$mol \cdot m^{-3} \cdot Pa^{-1} \cdot s^{-1}$
K	Equilibrium coefficient	$m^3 \cdot mol^{-1}$
l	Liquid molar flow rate	$mol \cdot s^{-1}$

L	Latent heat	J·mol^{-1}
M	Molar mass	mol·kg^{-1}
N_A	CO_2 mass transfer rate	mol·m^{-3}·s^{-1}
N_{HX}	Number of plates of cross-heat exchanger	
p	Pressure	Pa
q	Mass flow rate	kg s^{-1}
Q_{HX}	Heat exchanged in cross-heat exchanger	W
Q_R	Heat for CO_2 desorption	J·kg CO_2^{-1}
r	Reaction rate	mol·m^{-3}·s^{-1}
t	Dimension of time	s
T	Temperature	K
u	Liquid velocity	m·s^{-1}
U	Overall heat transfer coefficient	W·m^{-2}·s^{-1}
v	Vapour molar flow rate	mol·s^{-1}
V	Volume	m^3
x	Dimension of space	m
x_B	Amine concentration	mol amine·mol solvent^{-1}
Y_{CO2}	Amount of CO_2 in raw gas	m^3 CO_2·m^3 gas^{-1}
Z	Electric charge	
Greek symbols		
α	Amine loading	mol CO_2·mol amine^{-1}
δ	Depth for simulation	m
ΔH	Heat of absorption	J·mol CO_2^{-1}
Δq	Solvent mass cyclic capacity	kg CO_2·kg solvent^{-1}
ε	Dielectric permittivity	
η	Viscosity	Pa·s
λ	Thermal conductivity	W·m^{-1}·s^{-1}
ρ	Density	kg·m^{-3}
τ	Time for simulation	s
χ	Association parameter	
ψ	Empirical parameter for equilibrium shift	
Subscripts		

A	Referring to CO_2
ABS	Referring to the absorber column
B	Referring to the amine
C	Referring to amine carbamate
$CH4$	Referring to methane
D	Referring to protonated amine
dil	Referring to the diluent
i	Referring to initial value before absorption
HX	Referring to the cross-heat exchanger
L	Referring to the liquid phase
MAX	Referring to maximum temperature achieved in absorber column
R	Referring to the reboiler
V	Referring to the vapour phase
X	Referring to the stream leaving the cross-heat exchanger
Superscripts	
0	Referring to unloaded solvent
$*$	Referring to aqueous solvent
sat	Referring to saturation condition

Bibliography

(1) Heldebrant, D. J.; Koech, P. K.; Rousseau, R.; Glezakou, V. A.; Cantu, D.; Malhotra, D.; Zheng, F.; Whyatt, G.; Freeman, C. J.; Bearden, M. D. Are Water-Lean Solvent Systems Viable for Post-Combustion CO2 Capture? In *Energy Procedia*; Elsevier Ltd, 2017; Vol. 114, pp 756–763. https://doi.org/10.1016/j.egypro.2017.03.1218.

(2) Hwang, J.; Kim, J.; Lee, H. W.; Na, J.; Ahn, B. S.; Lee, S. D.; Kim, H. S.; Lee, H.; Lee, U. An Experimental Based Optimization of a Novel Water Lean Amine Solvent for Post Combustion CO2 Capture Process. *Appl. Energy* **2019**, *248*, 174–184. https://doi.org/10.1016/j.apenergy.2019.04.135.

(3) Leites, I. L. L. Thermodynamics of CO2 Solubility in Mixtures Monoethanolamine with Organic Solvents and Water and Commercial Experience of Energy Saving Gas Purification Technology. *Energy Convers. Manag.* **1998**, *39* (16–18), 1665–1674.

(4) Lail, M.; Tanthana, J.; Coleman, L. Non-Aqueous Solvent (NAS) CO2 Capture Process. *Energy Procedia* **2014**, *63*, 580–594. https://doi.org/10.1016/J.EGYPRO.2014.11.063.

(5) Yamamoto, S.; Yamada, H.; Higashii, T. Development of Chemical CO2 Solvent For High Pressure CO2 Capture (2): Addition Effects of Non-Aqueous Media on Amine Solutions. *Energy Procedia* **2014**, *63*, 1963–1971. https://doi.org/10.1016/J.EGYPRO.2014.11.209.

(6) Heldebrant, D. J.; Koech, P. K.; Glezakou, V.-A.; Rousseau, R.; Malhotra, D.; Cantu, D. C. Water-Lean Solvents for Post-Combustion CO2 Capture: Fundamentals, Uncertainties, Opportunities, and Outlook. **2017**. https://doi.org/10.1021/acs.chemrev.6b00768.

(7) Rivas, O. R.; Prausnitz, J. M. Sweetening of Sour Natural Gases by Mixed-Solvent Absorption: Solubilities of Ethane, Carbon Dioxide, and Hydrogen Sulfide in Mixtures of Physical and Chemical Solvents. *AIChE J.* **1979**, *25* (6), 975–984. https://doi.org/10.1002/aic.690250608.

(8) Roberts, B. E.; Mather, A. E. Solubility of CO2 and H2S in a Mixed Solvent. *Chem. Eng. Commun.* **1988**, *72* (1), 201–211. https://doi.org/10.1080/00986448808940017.

(9) Yuan, Y.; Rochelle, G. T. CO2 Absorption Rate in Semi-Aqueous Monoethanolamine. *Chem. Eng. Sci.* **2018**, *182*, 56–66. https://doi.org/10.1016/J.CES.2018.02.026.

(10) Wanderley, R. R.; Pinto, D. D. D.; Knuutila, H. K. Investigating Opportunities for Water-Lean Solvents in CO2 Capture: VLE and Heat of Absorption in Water-Lean Solvents Containing MEA. *Sep. Purif. Technol.* **2020**, *231*, 115883. https://doi.org/10.1016/j.seppur.2019.115883.

(11) Wanderley, R. R.; Evjen, S.; Pinto, D. D. D.; Knuutila, H. K. The Salting-out Effect in Some Physical Absorbents for CO2 Capture. In *Chemical Engineering Transactions*; 2018; Vol. 69, pp 97–102. https://doi.org/10.3303/CET1869017.

(12) Svensson, H.; Zejnullahu Velasco, V.; Hulteberg, C.; Karlsson, H. T. Heat of Absorption of Carbon Dioxide in Mixtures of 2-Amino-2-Methyl-1-Propanol and Organic Solvents. *Int. J. Greenh. Gas Control* **2014**, *30*, 1–8. https://doi.org/10.1016/J.IJGGC.2014.08.022.

(13) *The Purification of Technological Gases*, 2nd ed.; Semenova, T. A., Leites, I. L., Eds.;

Chimia: Moscow, 1977.

(14) Wanderley, R. R.; Yuan, Y.; Rochelle, G. T.; Knuutila, H. K. CO2 Solubility and Mass Transfer in Water-Lean Solvents. *Chem. Eng. Sci.* **2019**, *202*, 403–416. https://doi.org/10.1016/J.CES.2019.03.052.

(15) Yuan, Y.; Rochelle, G. T. Lost Work: A Comparison of Water-Lean Solvent to a Second Generation Aqueous Amine Process for CO 2 Capture. *Int. J. Greenh. Gas Control* **2019**, 82–90. https://doi.org/10.1016/j.ijggc.2019.03.013.

(16) Oexmann, J.; Kather, A. Minimising the Regeneration Heat Duty of Post-Combustion CO2 Capture by Wet Chemical Absorption: The Misguided Focus on Low Heat of Absorption Solvents. *Int. J. Greenh. Gas Control* **2010**, *4* (1), 36–43.

(17) Barzagli, F.; Lai, S.; Mani, F. Novel Non-Aqueous Amine Solvents for Reversible CO2 Capture. In *Energy Procedia*; Elsevier Ltd, 2014; Vol. 63, pp 1795–1804. https://doi.org/10.1016/j.egypro.2014.11.186.

(18) Sada, E.; Kumazawa, H.; Osawa, Y.; Matsuura, M.; Han, Z. Q. Reaction Kinetics of Carbon Dioxide with Amines in Non-Aqueous Solvents. *Chem. Eng. J.* **1986**, *33* (2), 87–95. https://doi.org/10.1016/0300-9467(86)80038-7.

(19) Sada, E.; Kumazawa, H.; Han, Z. Q.; Matsuyama, H. Chemical Kinetics of the Reaction of Carbon Dioxide with Ethanolamines in Nonaqueous Solvents. *AIChE J.* **1985**, *31* (8), 1297–1303. https://doi.org/10.1002/aic.690310808.

(20) Sada, E.; Kumazawa, H.; Han, Z. Q. Kinetics of Reaction between Carbon Dioxide and Ethylenediamine in Nonaqueous Solvents. *Chem. Eng. J.* **1985**, *31* (2), 109–115. https://doi.org/10.1016/0300-9467(85)80049-6.

(21) Versteeg, G. F.; Kuipers, J. A. M.; Van Beckum, F. P. H.; Van Swaaij, W. P. M. Mass Transfer with Complex Reversible Chemical Reactions—I. Single Reversible Chemical Reaction. *Chem. Eng. Sci.* **1989**, *44* (10), 2295–2310. https://doi.org/10.1016/0009-2509(89)85163-2.

(22) Versteeg, G. F.; Kuipers, J. A. M.; Van Beckum, F. P. H.; Van Swaaij, W. P. M. Mass Transfer with Complex Reversible Chemical Reactions-II. Parallel Reversible Chemical Reactions. *Chem. Eng. Sci.* **1990**, *45* (1), 183–197. https://doi.org/10.1016/0009-2509(90)87091-6.

(23) Danckwerts, P. V. The Reaction of CO2 with Ethanolamines. *Chem. Eng. Sci.* **1979**, *34* (4), 443–446. https://doi.org/10.1016/0009-2509(79)85087-3.

(24) Crooks, J. E.; Donnellan, J. P. Kinetics and Mechanism of the Reaction between Carbon Dioxide and Amines in Aqueous Solution. *J. Chem. Soc. Perkin Trans. 2* **1989**, No. 4, 331–333. https://doi.org/10.1039/p29890000331.

(25) Da Silva, E. F.; Svendsen, H. F. Ab Initio Study of the Reaction of Carbamate Formation from CO2 and Alkanolamines. *Ind. Eng. Chem. Res.* **2004**, *43* (13), 3413–3418. https://doi.org/10.1021/ie030619k.

(26) Hartono, A.; Svendsen, H. F. Kinetics Reaction of Primary and Secondary Amine Group in Aqueous Solution of Diethylenetriamine (DETA) with Carbon Dioxide. In *Energy Procedia*; 2009; Vol. 1, pp 853–859. https://doi.org/10.1016/j.egypro.2009.01.113.

(27) Sherman, B. J.; Rochelle, G. T. Thermodynamic and Mass-Transfer Modeling of Carbon Dioxide Absorption into Aqueous 2-Amino-2-Methyl-1-Propanol. *Ind. Eng. Chem. Res.* **2017**, *56* (1), 319–330. https://doi.org/10.1021/acs.iecr.6b03009.

(28) Rocha, J. A.; Bravo, J. L.; Fair, J. R. *Distillation Columns Containing Structured Packings: A Comprehensive Model for Their Performance. 1. Hydraulic Models*; 1993; Vol. 32.

(29) Rocha, J. A.; Bravo, J. L.; Fair, J. R. *Distillation Columns Containing Structured Packings: A Comprehensive Model for Their Performance. 2. Mass-Transfer Model*; 1996; Vol. 35.

(30) Wilke, C. R.; Chang, P. Correlation of Diffusion Coefficients in Dilute Solutions. *AIChE J.* **1955**, *1* (2), 264–270. https://doi.org/10.1002/aic.690010222.

(31) Versteeg, G. F.; van Swaal, W. P. M. Solubility and Diffusivity of Acid Gases (CO2, N2O) in Aqueous Alkanolamine Solutions. *J. Chem. Eng. Data* **1988**, *33* (1), 29–34. https://doi.org/10.1021/je00051a011.

(32) Dugas, R. E.; Rochelle, G. T. Modeling CO2 Absorption into Concentrated Aqueous Monoethanolamine and Piperazine. *Chem. Eng. Sci.* **2011**, *66* (21), 5212–5218. https://doi.org/10.1016/j.ces.2011.07.011.

(33) Park, S.; Lee, J.; Choi, B.; Lee, J. Reaction Kinetics of Carbon Dioxide with Diethanolamine in Polar Organic Solvents. *Sep. Sci. Technol.* **2005**, *40* (9), 1885–1898.

https://doi.org/10.1081/SS-200064536.

(34) Hwang, K.-S.; Park, S.-W.; Park, D.-W.; Oh, K.-J.; Kim, S.-S. Absorption of Carbon Dioxide into Diisopropanolamine Solutions of Polar Organic Solvents. *J. Taiwan Inst. Chem. Eng.* **2010**, *41* (1), 16–21. https://doi.org/10.1016/J.JTICE.2009.05.009.

(35) Snijder, E. D.; Te Riele, M. J. M.; Versteeg, G. F.; Van Swaaij, W. P. M. Diffusion Coefficients of Several Aqueous Alkanolamine Solutions. **1993**, *38* (3), 475–480. https://doi.org/10.1021/je00011a037.

(36) Park, S. W.; Lee, J. W.; Choi, B. S.; Lee, J. W. Absorption of Carbon Dioxide into Non-Aqueous Solutions of N-Methyldiethanolamine. *Korean J. Chem. Eng.* **2006**, *23* (5), 806–811. https://doi.org/10.1007/BF02705932.

(37) Fialkov, Y. Y.; Chumak, V. L. Solvent Mixtures. In *Handbook of Solvents: Second Edition*; Elsevier Inc., 2014; Vol. 1, pp 403–465. https://doi.org/10.1016/B978-1-895198-64-5.50012-X.

(38) Sen, B.; Roy, R. N.; Gibbons, J. J.; Johnson, D. A.; Adcock, L. H. Computational Techniques of Ionic Processes in Water—Organic Mixed Solvents; 1979; pp 215–248. https://doi.org/10.1021/ba-1979-0177.ch015.

(39) Aronu, U. E.; Lauritsen, K. G.; Grimstvedt, A.; Mejdell, T. Impact of Heat Stable Salts on Equilibrium CO2 Absorption. In *Energy Procedia*; Elsevier Ltd, 2014; Vol. 63, pp 1781–1794. https://doi.org/10.1016/j.egypro.2014.11.185.

(40) Browning, G. J.; Weiland, R. H. Physical Solubility of Carbon Dioxide in Aqueous Alkanolamines via Nitrous Oxide Analogy. *J. Chem. Eng. Data* **1994**, *39* (4), 817–822. https://doi.org/10.1021/je00016a040.

(41) Guo, H.; Hui, L.; Shen, S. Monoethanolamine+2-Methoxyethanol Mixtures for CO2 Capture: Density, Viscosity and CO2 Solubility. *J. Chem. Thermodyn.* **2019**, *132*, 155–163. https://doi.org/10.1016/j.jct.2018.12.028.

(42) Esteves, M. J. C.; Cardoso, M. J. E. de M.; Barcia, O. E. A Debye−Hückel Model for Calculating the Viscosity of Binary Strong Electrolyte Solutions. *Ind. Eng. Chem. Res.* **2001**, *40* (22), 5021–5028. https://doi.org/10.1021/ie010392y.

(43) Lee, J. I.; Otto, F. D.; Mather, A. E. The Solubility of Mixtures of Carbon Dioxide and Hydrogen Sulphide in Aqueous Diethanolamine Solutions. *Can. J. Chem. Eng.* **1974**, *52*

(1), 125–127. https://doi.org/10.1002/cjce.5450520121.

(44) Yuan, Y.; Rochelle, G. T. CO2 Absorption Rate and Capacity of Semi-Aqueous Piperazine for CO2 Capture. *International Journal of Greenhouse Gas Control*. Elsevier Ltd June 1, 2019, pp 182–186. https://doi.org/10.1016/j.ijggc.2019.03.007.

(45) Wang, L.; Zhang, Y.; Wang, R.; Li, Q.; Zhang, S.; Li, M.; Liu, J.; Chen, B. Advanced Monoethanolamine Absorption Using Sulfolane as a Phase Splitter for CO2 Capture. *Environ. Sci. Technol.* **2018**, *52* (24), 14556–14563. https://doi.org/10.1021/acs.est.8b05654.

(46) Vaidya, P. D.; Mahajani, V. V. Kinetics of the Reaction of CO2 with Aqueous Formulated Solution Containing Monoethanolamine, N-Methyl-2-Pyrrolidone, and Diethylene Glycol. *Ind. Eng. Chem. Res.* **2005**, *44* (6), 1868–1873. https://doi.org/10.1021/ie049226r.

(47) Seader, J. D.; Henley, E. J.; Roper, D. K. *Separation Process Principles with Applications Using Process Simulators*, 3rd ed.; Wiley, 2010.

(48) Ryckebosch, E.; Drouillon, M.; Vervaeren, H. Techniques for Transformation of Biogas to Biomethane. *Biomass and Bioenergy* **2011**, *35* (5), 1633–1645. https://doi.org/10.1016/J.BIOMBIOE.2011.02.033.

(49) Kvamsdal, H. M.; Rochelle, G. T. Effects of the Temperature Bulge in CO 2 Absorption from Flue Gas by Aqueous Monoethanolamine. **2008**. https://doi.org/10.1021/ie061651s.

(50) Kim, I.; Svendsen, H. F. Heat of Absorption of Carbon Dioxide (CO2) in Monoethanolamine (MEA) and 2-(Aminoethyl)Ethanolamine (AEEA) Solutions. **2007**. https://doi.org/10.1021/IE0616489.

(51) Kim, I.; Hoff, K. A.; Mejdell, T. Heat of Absorption of CO2 with Aqueous Solutions of MEA: New Experimental Data. *Energy Procedia* **2014**, *63*, 1446–1455. https://doi.org/10.1016/J.EGYPRO.2014.11.154.

(52) Kriebel, M. Improved Amisol Process for Gas Purification. *Energy Prog.; (United States)* **1984**, *4:3*.

(53) Kohl, A. L.; Nielsen, R. B.; Kohl, A. L.; Nielsen, R. B. Physical Solvents for Acid Gas Removal. *Gas Purif.* **1997**, 1187–1237. https://doi.org/10.1016/B978-088415220-

0/50014-8.

(54) Xu, M.; Wang, S.; Xu, L. Screening of Physical-Chemical Biphasic Solvents for CO2 Absorption. *Int. J. Greenh. Gas Control* **2019**, *85*, 199–205. https://doi.org/10.1016/j.ijggc.2019.03.015.

(55) Lin, Y. J.; Rochelle, G. T. Heat Transfer Enhancement and Optimization of Lean/Rich Solvent Cross Exchanger for Amine Scrubbing. In *Energy Procedia*; Elsevier Ltd, 2017; Vol. 114, pp 1890–1903. https://doi.org/10.1016/j.egypro.2017.03.1320.

(56) Dhar, P. L. Modeling of Thermal Equipment. In *Thermal System Design and Simulation*; Elsevier, 2017; pp 147–296. https://doi.org/10.1016/b978-0-12-809449-5.00004-8.

(57) Okada, K.; Ono, M.; Tomimura, T.; Okuma, T.; Konno, H.; Ohtani, S. Design and Heat Transfer Characteristics of New Plate Heat Exchanger. *Heat Transf. - Japanese Res.* **1972**, *1* (1), 90–95.

(58) Høisæter, K. K.; Knuutila, H. K. Degradation potential of aqueous and water-lean MEA https://az659834.vo.msecnd.net/eventsairwesteuprod/production-ieaghg-public/8b35e3179849420384cc66fc8223bbf3 (accessed Dec 12, 2019).

(59) Frimpong, R. A.; Remias, J. E.; Neathery, J. K.; Liu, K. Solvent Regeneration with a High Volatility Liquid as Stripping Carrier. *Int. J. Greenh. Gas Control* **2012**, *9*, 124–129. https://doi.org/10.1016/j.ijggc.2012.03.014.

(60) Barbosa, L. C.; Araújo, O. de Q. F.; de Medeiros, J. L. Carbon Capture and Adjustment of Water and Hydrocarbon Dew-Points via Absorption with Ionic Liquid [Bmim][NTf2] in Offshore Processing of CO2-Rich Natural Gas. *J. Nat. Gas Sci. Eng.* **2019**, *66*, 26–41. https://doi.org/10.1016/j.jngse.2019.03.014.

(61) Wang, Y.; Liu, X.; Kraslawski, A.; Gao, J.; Cui, P. A Novel Process Design for CO 2 Capture and H 2 S Removal from the Syngas Using Ionic Liquid. *J. Clean. Prod.* **2019**, *213*, 480–490. https://doi.org/10.1016/j.jclepro.2018.12.180.

(62) Basha, O. M.; Keller, M. J.; Luebke, D. R.; Resnik, K. P.; Morsi, B. I. Development of a Conceptual Process for Selective CO2 Capture from Fuel Gas Streams Using [Hmim][Tf2N] Ionic Liquid as a Physical Solvent. *Energy and Fuels* **2013**, *27* (7), 3905–3917. https://doi.org/10.1021/ef400650w.

(63) Li, L.; Huang, X.; Jiang, Q.; Xia, L.; Wang, J.; Ai, N. New Process Development and

Process Evaluation for Capturing CO2 in Flue Gas from Power Plants Using Ionic Liquid [Emim][Tf2N]. *Chinese J. Chem. Eng.* **2020**. https://doi.org/10.1016/j.cjche.2019.08.005.

(64) Bara, J. E.; Mittenthal, M. S.; Flowers, B.; Taylor, W. F.; Jenkins, A. H.; Wallace, D. A.; David Roveda, J. Lessons Learned from the Use of Unconventional Materials for CO2 Capture. In *MRS Advances*; Materials Research Society, 2016; Vol. 1, pp 3027–3035. https://doi.org/10.1557/adv.2016.496.

(65) Guo, H.; Li, C.; Shi, X.; Li, H.; Shen, S. Nonaqueous Amine-Based Absorbents for Energy Efficient CO2 Capture. *Appl. Energy* **2019**, *239*, 725–734. https://doi.org/10.1016/j.apenergy.2019.02.019.

(66) Sprung, M. A. A Summary of the Reactions of Aldehydes with Amines. *Chem. Rev.* **1940**, *26* (3), 297–338. https://doi.org/10.1021/cr60085a001.

(67) Moser, P.; Schmidt, S.; Sieder, G.; Garcia, H.; Stoffregen, T. Performance of MEA in a Long-Term Test at the Post-Combustion Capture Pilot Plant in Niederaussem. *Int. J. Greenh. Gas Control* **2011**, *5* (4), 620–627. https://doi.org/10.1016/j.ijggc.2011.05.011.

(68) Moser, P.; Wiechers, G.; Schmidt, S.; Elsen, R.; Goetheer, E.; Khakharia, P.; Monteiro, J. G. M.-S.; Jens, K.-J.; Solli, K.-A.; Fernandez, E. S.; et al. MEA consumption – ALIGN-CCUS: Comparative long-term testing to answer the open questions https://papers.ssrn.com/sol3/papers.cfm?abstract_id=3366052 (accessed Jan 6, 2020).

(69) Smith, M. *March's Advanced Organic Chemistry : Reactions, Mechanisms, and Structure.*

(70) Karlsson, H. K.; Drabo, P.; Svensson, H. Precipitating Non-Aqueous Amine Systems for Absorption of Carbon Dioxide Using 2-Amino-2-Methyl-1-Propanol. *Int. J. Greenh. Gas Control* **2019**, *88*, 460–468. https://doi.org/10.1016/j.ijggc.2019.07.001.

(71) Wang, R.; Liu, S.; Wang, L.; Li, Q.; Zhang, S.; Chen, B.; Jiang, L.; Zhang, Y. Superior Energy-Saving Splitter in Monoethanolamine-Based Biphasic Solvents for CO2 Capture from Coal-Fired Flue Gas. *Appl. Energy* **2019**, *242*, 302–310. https://doi.org/10.1016/j.apenergy.2019.03.138.

(72) Luo, W.; Guo, D.; Zheng, J.; Gao, S.; Chen, J. CO2 Absorption Using Biphasic Solvent: Blends of Diethylenetriamine, Sulfolane, and Water. *Int. J. Greenh. Gas Control* **2016**,

53, 141–148. https://doi.org/10.1016/j.ijggc.2016.07.036.

Table of contents

An in-depth assessment of solvent properties for designing better water-lean solvents